In vivo *studies*

OT-7100 was suspended in polyethylene glycol 400 for intravenous administration and in 5% acacia solution for oral administration. The animals were fasted for 20 h before OT-7100 administration. OT-7100 was administered orally at doses of 30, 100 and 1000 mg kg^{-1} to rats, dogs and monkeys, respectively, and intravenously at the same dose of 5 mg kg^{-1} to rats, dogs and monkeys. OT-7100 was administered at 09:00 h. All treated animals were given access to food at 11:00 h and were allowed free access to tap water. Heparinized samples of whole blood were obtained from rats, dogs and monkeys at several time points after administration (Figure 2) (24 h was the last sampling tine after oral and intravenous administration). Plasma samples were separated from whole blood by centrifuging the blood samples at 1800*g* for 10 min at 4°C and were stored frozen at −20°C until the analyses were performed.

OT-7100 and its metabolites in the plasma were assayed using a validated high-performance liquid chromatography (HPLC) method. Briefly, a 0.3-ml aliquot of each plasma sample was first added to 0.9 ml acetonitrile. After centrifugation at 10 000*g* for 15 min at 4°C, the supernatant (0.9 ml) was transferred to another tube and dried under nitrogen at 40°C. The residue was dissolved in 0.5 ml of a mixture of acetonitrile and potassium phosphate buffer (10 mM, pH 5.5) at a ratio of 1:3 (v/v) and 0.2 ml of this suspension were then injected onto the HPLC.

In vitro *metabolic studies of OT-7100*

The hydroxylase activities towards OT-7100 were determined by quantifying the formation of M19 (Figure 1). A 0.1-ml aliquot of cytosol and microsomes from the liver and small intestine of rats, dogs, monkeys and humans (approximately 10 mg protein ml^{-1}) was added to 0.89 ml 0.1 M Na-K phosphate buffer (pH 7.4). The reaction was started by adding 10 µl substrate (1000 µg ml^{-1} acetonitrile) after pre-incubation for 5 min at 37°C. The reaction was stopped by adding 2.0 ml acetonitrile after incubation for 30 min at 37°C. The reaction mixture was then centrifuged at 3000 rpm for 10 min at 4°C. The resulting supernatant (1.0 ml) was evaporated under a nitrogen stream at 40°C. The residue was dissolved in 0.5 ml of a mixture of acetonitrile and potassium phosphate buffer (10 mM, pH 5.5) at a ratio of 1:3 (v/v) and a 0.2-ml aliquot was injected onto the HPLC.

HPLC analysis of OT-7100 and metabolites

OT-7100 and its metabolites were assayed using a HPLC method validated over a concentration range of 0.01–1.00 µg ml^{-1}. OT-7100 and its metabolites were separated on a 250 × 4.6 mm i.d. Inertsil ODS-3V column (GL-Sciences, Tokyo, Japan) and detected at wavelengths of 215 nm (for M19) and 230 nm (for OT-7100 and the other four metabolites) using an HPLC system (LC-10A Series, Shimadzu, Kyoto, Japan). OT-7100 and the metabolites were eluted at a flow rate of 1.0 ml min^{-1} with 10 mM potassium buffer (pH 5.5)/acetonitrile according to the following gradient schedule: 33% acetonitrile for the first 3 min; a linear gradient from 33 to 40% over the next 7 min; a linear gradient from 40 to 50% over the next 4 min; a linear gradient from 50 to 64% over the next 6 min; a linear gradient from 64 to 68% over the next 3 min; and a linear gradient from 68 to 70% over the next 9 min, which was then finally maintained at 80% for 10 min. The temperature of the column was maintained at 40°C.

Data analysis

The OT-7100 concentrations at time 0 (C_0) were extrapolated from the initial slope. The maximum concentrations (C_{max}) and the times to reach the maximum concentration (T_{max}) were read directly from the mean concentration data. The elimination half-lives ($t_{1/2}$) were estimated as $\ln 2/k$, where k is the slope of the terminal linear portion of the semi-logarithmic plasma concentration–time curve. The areas under the plasma concentration–time curves from time 0 to the last detectable concentration (AUC_{0-t}) and the mean residence times (MRT) were calculated using the trapezoidal rule (Yamaoka et al. 1978). Total systemic clearances (CL_{tot}) and volume of distribution at steady state (V_{dss}) were calculated according to the following equations:

$$CL_{tot} = \frac{D_{i.v.}}{AUC_{0-t}}$$

$$V_{dss} = D_{i.v.} \cdot \frac{MRT}{AUC},$$

where $D_{i.v.}$ is the administered dose. The absolute bioavailability (BA) was calculated as:

$$D_{i.v.} \cdot \frac{AUC_{p.o.}}{D_{p.o.}} \cdot AUC_{i.v.}$$

of OT-7100 in the plasma and expressed as a percentage. The AUC_{0-t} values of OT-7100 after oral administration were normalized for the dose levels divided by $mg\,kg^{-1}$.

Statistical analysis

All graphical data are the mean ± SD. Analysis of statistical significance, where appropriate, was performed by the Tukey's test using the statistical package program SAS® System 8.2 (SAS Institute, Inc., Cary, NC, USA).

Results

Species differences in the pharmacokinetics of OT-7100 and its metabolites in rats, dogs and monkeys

The plasma concentration–time profiles of OT-7100 after oral and intravenous administration of OT-7100 to rats, dogs and monkeys are shown in Figure 2 and the pharmacokinetic parameters are summarized in Table I. The plasma concentration–time profiles of OT-7100 were also normalized to a dose of $1\,mg\,kg^{-1}$ (Figure 3).

OT-7100 was administered orally at doses of 30, 100 and $1000\,mg\,kg^{-1}$ to rats, dogs and monkeys, respectively. The C_{max} values for OT-7100 in rats, dogs and monkeys were 0.58, 0.36 and $0.16\,\mu g\,ml^{-1}$, respectively. The $t_{1/2}$ values of OT-7100 in rats, dogs and monkeys were 3.1, 6.2 and 3.6 h, respectively. OT-7100 was not detected in monkey plasma at 24 h after oral administration. The oral bioavailabilities of OT-7100 were calculated from the AUC_{0-t} by normalizing for oral and intravenous administration dose concentrations. The bioavailabilities of OT-7100 in rats, dogs and monkeys were 36, 17 and 0.3%, respectively. In the preliminary experiments, the C_{max} values of OT-7100 in monkey plasma after oral administration increased dose-dependently for doses of 300–$1000\,mg\,kg^{-1}$,

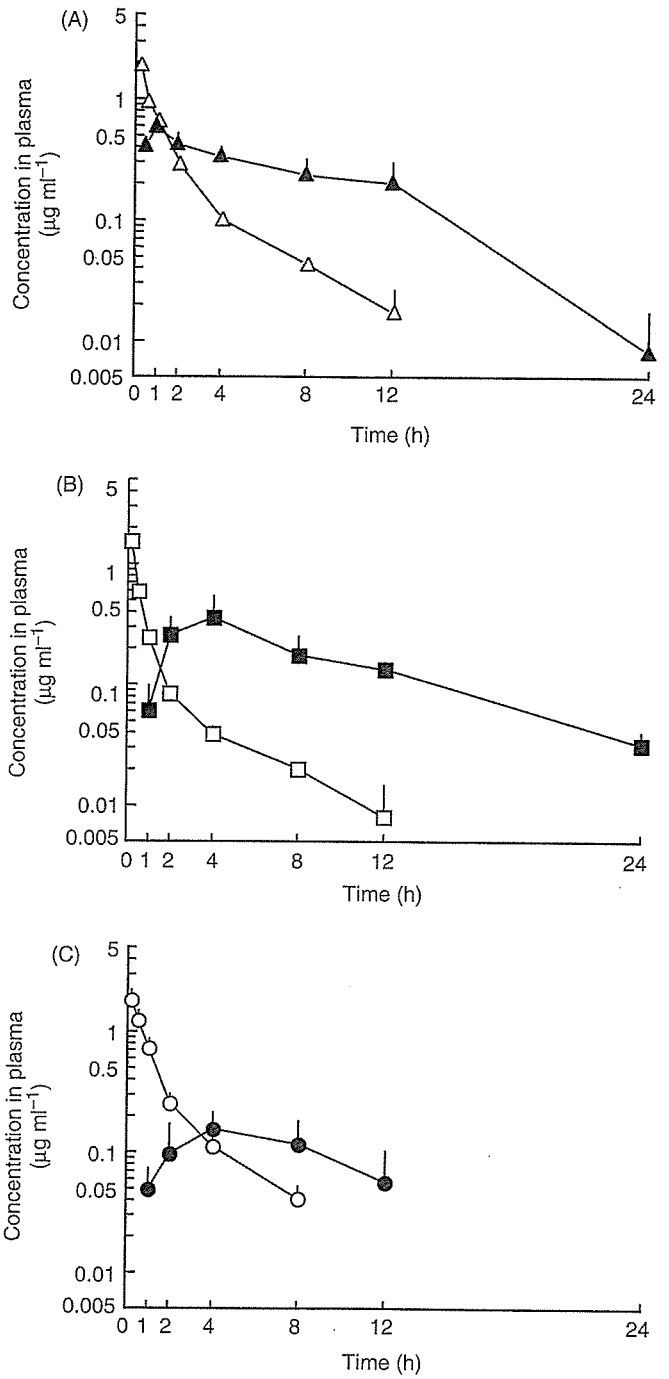

Figure 2. Plasma concentrations of OT-7100 in rats (A), dogs (B) and monkeys (C) after oral (closed symbols) and intravenous (open symbols) administration of OT-7100. OT-7100 was administered orally at a dose of 30 mg kg^{-1} in rats, 100 mg kg^{-1} in dogs and 1000 mg kg^{-1} in monkeys, and intravenously at a dose of 5 mg kg^{-1} in all species. Data are the mean ± SD of three to five animals.

Table I. Pharmacokinetic parameters of OT-7100 in plasma after oral and intravenous administration of OT-7100 to rats, dogs and monkeys.

Species	Rat	Dog	Monkey
Oral administration			
Dose ($mg\,kg^{-1}$)	30	100	1000
C_{max} ($\mu g\,ml^{-1}$)	0.58 ± 0.07	0.36 ± 0.19	0.16 ± 0.06
T_{max} (h)	1.0	4.0	5.3
$t_{1/2}$ (h)	3.1	6.2	3.6
AUC_{0-t} ($\mu g\,h\,ml^{-1}$)	4.88	3.83	1.47
Normalized AUC_{0-t} ($\mu g\,h\,ml^{-1}$)	0.163	0.0383	0.00147
BA (%)	36	17	0.3
Intravenous administration			
Dose ($mg\,kg^{-1}$)	5.0	5.0	5.0
C_0 ($\mu g\,ml^{-1}$)	2.05	2.03	2.13
$t_{1/2}(\alpha)$ (h)	0.6	0.3	0.7
$t_{1/2}(\beta)$ (h)	3.4	3.9	2.4
AUC_{0-t} ($\mu g\,h\,ml^{-1}$)	2.28	1.17	2.51
CL_{tot} ($l\,h^{-1}\,kg^{-1}$)	2.0	3.9	1.9
V_{dss} ($l\,kg^{-1}$)	4.8	7.7	3.8
MRT (h)	2.4	2.1	2.0

C_0, plasma concentration at time 0; C_{max}, maximum concentration; T_{max}, time to maximum concentration; $t_{1/2}$, elimination half-life; AUC_{0-t}, area under the plasma concentration–time curve from 0 to the last measurement point; CL_{tot}, clearance = dose/AUC_{0-t}; V_{dss}, volume of distribution; MRT, mean residence time; BA, bioavailability. Data are calculated from the means obtained from five rats, three dogs and three monkeys. C_{max} is mean ± SD of five rats, three dogs and three monkeys.

and OT-7100 bioavailability was the same for doses of 300–1000 $mg\,kg^{-1}$. OT-7100 concentrations in the plasma normalized for oral administered dose concentrations were highest in rats, moderate in dogs and lowest in monkeys. The OT-7100 AUC_{0-t} values normalized for dose levels in rats, dogs and monkeys were 0.163, 0.0383 and 0.00147 $\mu g\,h\,ml^{-1}$ divided by $mg\,kg^{-1}$, respectively. The normalized AUC_{0-t} values of OT-7100 in monkeys were lower than those in dogs and rats (approximately 1/25 of AUC_{0-t} in dogs and 1/100 of AUC_{0-t} in rats).

After intravenous administration of OT-7100 at a dose of 5 $mg\,kg^{-1}$, the plasma concentration–time profiles of OT-7100 in rats, dogs and monkeys were similar. The C_0 values of OT-7100 in rats, dogs and monkeys were 2.05, 2.03 and 2.13 $\mu g\,ml^{-1}$, respectively. The $t_{1/2}(\alpha)$ values of OT-7100 were 0.6 h in rats and 0.7 h in monkeys. OT-7100 was not detected in the plasma of rats, dogs and monkeys at 24 h and in monkey plasma at 12 h after intravenous administration. The AUC_{0-t} values were 2.28 $\mu g\,h\,ml^{-1}$ in rats and 2.51 $\mu g\,h\,ml^{-1}$ in monkeys. In contrast, the $t_{1/2}(\alpha)$ values (0.3 h) of OT-7100 in dog plasma were half of those in rats and monkeys, indicating that the OT-7100 concentrations in dog plasma were eliminated more rapidly and were lower than those in rats and monkeys. The AUC_{0-t} values (1.17 $\mu g\,h\,ml^{-1}$) of OT-7100 in dog plasma were equivalent to approximately 50% of those for rats and monkeys. The CL_{tot} values of OT-7100 in rats, dogs and monkeys were 2.0, 3.9 and 1.9 $l\,h^{-1}\,kg^{-1}$, respectively. The V_{dss} values of OT-7100 in rats, dogs and monkeys were 4.8, 7.7 and 3.8 $l\,kg^{-1}$, respectively.

As shown in Figure 1, the main metabolic pathway of OT-7100 is hydrolysis of the amide moiety (by esterases) to M19 and M5. In the preliminary experiments, M5 was rapidly converted via phase II metabolism to glucuronide and sulfate conjugates and excreted

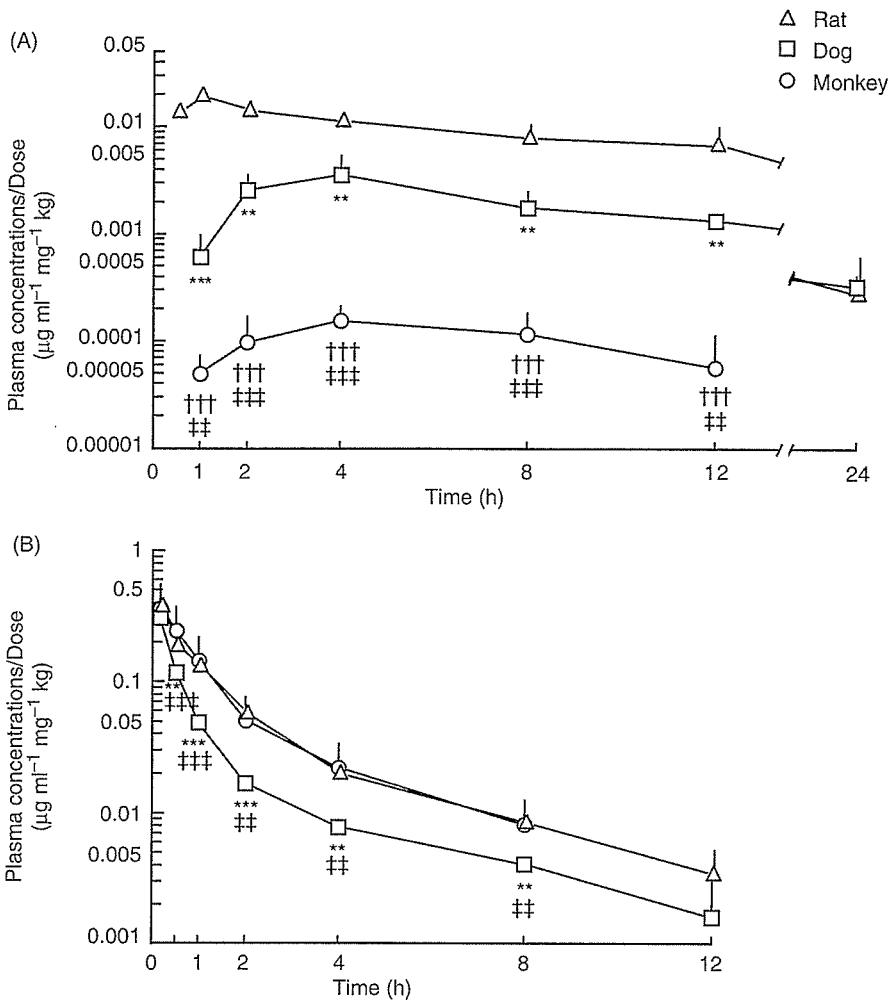

Figure 3. Dose-normalized plasma concentrations–time profiles for OT-7100 in rats, dogs and monkeys after oral (A) and intravenous (B) administration of OT-7100. Data normalized for dose (1 mg kg^{-1}) are expressed as the mean ± SD of three to five animals. Values were significantly different at $^{**}p < 0.01$ and $^{***}p < 0.001$ between rat and dog, at $\dagger\dagger\dagger p < 0.001$ between rat and monkey, and at $\ddagger\ddagger p < 0.01$ and $\ddagger\ddagger\ddagger p < 0.001$ between dog and monkey.

into urine and bile, respectively (data not shown). Since M19 does not readily undergo phase II metabolism (data not shown), it is reasonable to estimate the hydrolase activities toward OT-7100 by quantifying this metabolite. The AUC_{0-t} values of OT-7100 and metabolites are summarized in Table II. After intravenous administration in rats, the AUC_{0-t} values of M19 (formed by hydrolysis of the OT-7100 amide moiety, 10.7 nmol h ml^{-1}) were 1.8 times higher than OT-7100 values. In contrast, after oral administration at a dose of 30 mg kg^{-1} in rats, the AUC_{0-t} values of M19 (66.9 nmol h ml^{-1}) were 5.3 times higher than OT-7100 values. Thus, M19 was determined to be the major metabolite of OT-7100 in rat plasma. In rats, in addition to M19, small amounts of M5 (formed by hydrolysis of the OT-7100 amide moiety) and M1–3 (formed by oxidation of the *n*-butyl groups) were also detected in the plasma. On the other hand, after intravenous

Table II. AUC_{0-t} values of OT-7100 and metabolites in plasma after oral and intravenous administration of OT-7100 to rats and dogs.

Species	Rat	Dog
Oral administration		
Dose ($mg\,kg^{-1}$)	30	100
AUC_{0-t} ($nmol\,h\,ml^{-1}$)		
OT-7100	12.7	10.0
M19	66.9	1812.6
M1	17.7	5.1
M2	3.9	8.8
M3	1.8	n.d.
M5	n.d.	n.d.
Intravenous administration		
Dose ($mg\,kg^{-1}$)	5	5
AUC_{0-t} ($nmol\,h\,ml^{-1}$)		
OT-7100	5.9	3.0
M19	10.7	190.9
M1	2.5	n.d.
M2	0.6	0.5
M3	0.1	n.d.
M5	0.2	n.d.

Metabolite concentrations in monkey plasma were not determined. Data are means obtained from five rats and three dogs. n.d., Not detected.
Molecular weight: M19, 212.20; M1, 416.44; M2, 400.44; M3, 400.44; M5, 190.25.

administration at a dose of $5\,mg\,kg^{-1}$ to dogs, the AUC_{0-t} values of M19 were 190.9 $nmol\,h\,ml^{-1}$, 63.6 times higher than OT-7100 values. After oral administration to dogs, the AUC_{0-t} values of M19 were 1812.6 nmol h ml^{-1}, and were 181.3 times higher than OT-7100 values. Therefore, M19 was also the major metabolite of OT-7100 in dog plasma (Table II).

Comparison of hydrolase activities toward OT-7100 in the liver and small intestine of rats, dogs, monkeys and humans

To elucidate species difference in the hydrolysis of OT-7100, an *in vitro* metabolic study was conducted using liver and small intestinal fractions obtained from rats, dogs, monkeys and humans. Since M19 was determined to be the major OT-7100 metabolite in rats and dogs, hydrolase activities toward OT-7100 were measured based on M19 production (Figure 4).

The hydrolase activities in liver cytosol were similar in all species ($4.6\,ng\,mg\,protein^{-1}\,min^{-1}$ in humans; $3.6–3.8\,ng\,mg\,protein^{-1}\,min^{-1}$ in other animals), indicating that there were no species differences in the hydrolysis of OT-7100 in liver cytosol. In contrast, the hydrolase activities in liver microsomes were 14.8, 19.7 and $14.7\,ng\,mg\,protein^{-1}\,min^{-1}$ in rats, dogs and monkeys, respectively. In human liver microsomes, the hydrolase activity ($4.3\,ng\,mg\,protein^{-1}\,min^{-1}$) was lower than those in the other animal species.

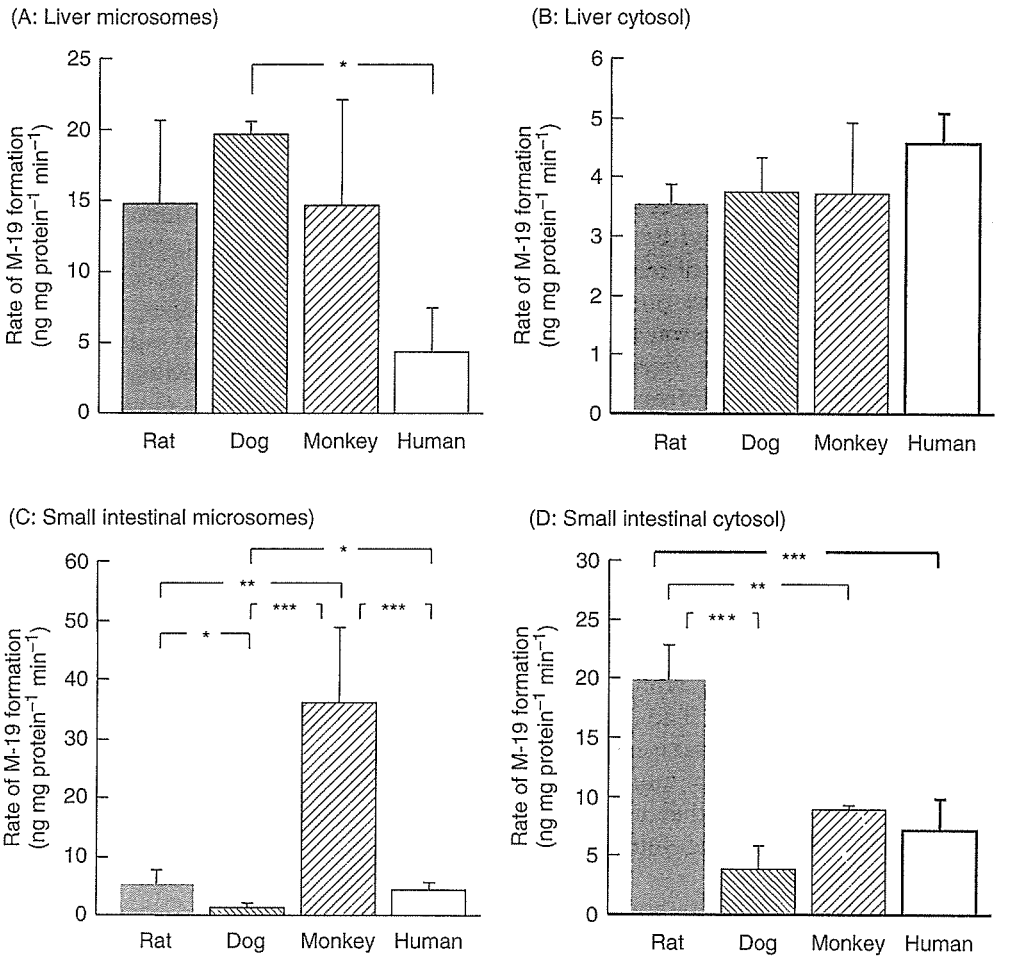

Figure 4. Hydrolase activities toward OT-7100 in liver and small intestinal fractions from rats, dogs, monkeys and humans. Data are the mean ± SD of three lots for rat small intestinal fractions (one lot was prepared from five animals) and three individuals for other fractions. The bracketed pairs of values are significantly different at $*p<0.05$, $**p<0.01$ and $***p<0.001$.

The small intestinal cytosolic hydrolase activities towards OT-7100 in rats (20.0 ng mg protein^{-1} min^{-1}) were significantly the highest, followed by monkeys, humans and dogs. The hydrolase activities determined using small intestinal microsomes from monkeys were 36.1 ng mg protein^{-1} min^{-1}, and were approximately eight, seven and 26 times higher than humans, rats and dogs, respectively. The hydrolase activities toward OT-7100 in dog small intestinal cytosol were approximately one-fifth of those in rats.

Discussion

It is important that first-pass metabolism influences are fully determined to estimate properly the biotransformation of orally administered drugs. The influence of the first-pass

effect in small intestines was investigated herein using OT-7100, a pyrazolopyrimidine derivative, as a probe drug with the amide moiety.

Carboxylesterases play an important role in the metabolic activation of prodrugs and can be classified into four families: CES 1–4 (Satoh and Hosokawa 1998). Various carboxylesterases are expressed in a wide variety of organs and tissues such as the liver, plasma, lung, kidney and brain in addition to the small intestine (Boogaard et al. 1999; Hosokawa et al. 2001; Zhang et al. 2002). Hydrolase activities can be induced by treatment with chemicals and inhibited by a variety of compounds (Morgan et al. 1994a; Yan et al. 1999; Zhu et al. 2000). Until recently, there were only a few reports on species differences in liver hydrolase activities, but the data now available are informative. For example, the hydrolase activities toward *para*-nitrophenylacetate in rat liver microsomes are approximately three times higher than those of dogs in the following order: rat $\geq$ monkey = human > dog (Morgan et al. 1994b). The hydrolase activities toward isocarboxazid in monkey liver microsomes are approximately 2.5 times higher than those of rats in the following order: monkey > dog $\geq$ rat > human. Moreover, the hydrolase activities toward butanilicaine in dog liver microsomes are approximately nine times higher than rats (Hosokawa et al. 1990). The hydrolase activities toward *O*-butyryl propranolol in dog liver microsomes are approximately twice higher than those of rats (Imai et al. 2003). Therefore, species differences in hydrolase activities by esterases differ widely from substrate to substrate.

In the present study, the hydrolase activities toward OT-7100 in liver cytosol were similar in all species tested. The hydrolyzing activities in dog liver microsomes were higher than those in rats and monkeys. The *in vitro* hydrolase activities in liver microsomes correlated with CL_{tot} and V_{dss} (dog > rat = monkey; Table I), and inversely correlated with OT-7100 plasma concentrations (rat = monkey > dog; Figure 3A) after intravenous administration. These result demonstrate that hydrolysis in the liver is one of the major contributions to the biotransformation of intravenously administered drugs with the amide moiety such as OT-7100.

Compared with data on carboxylesterases in the liver, there are few reports on species differences for hydrolysis by carboxylesterases in the small intestine. Inoue et al. (1979) examined hydrolase activities for several substrates using homogenates of intestinal mucosa from six species (human, rat, mouse, guinea pig, rabbit and dog), and reported a difference in the substrate specificity of the intestinal esterase from mice and rats, which hydrolysed esters better compared with the other species. The same study reported that hydrolase activities from dog intestine, tested using several esters as substrates, were low (Inoue et al. 1979). Furthermore, the *in vitro* hydrolysis rate in small intestinal mucosa for glycovir, a perbutyrylated ester prodrug of SC-48334, was highest in rats, moderate in monkeys and humans, and lowest in dogs, which was also reflected in the order of decreasing relative bioavailability of active SC-48334 (Cook et al. 1995).

In the present study, hydrolase activities toward OT-7100 in small intestinal cytosol were highest in rats, moderate in monkeys and humans, and lowest in dogs, consistent with Cook et al. (1995). In contrast, our findings on the rank order of hydrolase activities in small intestinal microsomes are not consistent with previous studies. The hydrolase activities in small intestinal microsomes from monkeys were seven, eight and 26 times higher than those of rats, humans and dogs, respectively. Therefore, species differences in hydrolase activities in the small intestinal microsomes varied more widely compared with those within the liver.

The results also demonstrate that the highest activity of OT-7100 hydrolysis in small intestinal microsomes from monkeys is one factor accounting for the poor oral bioavailability

in monkeys (0.3%). This conclusion is also supported by the species differences observed in OT-7100 plasma concentration–time profiles normalized for dose concentration after oral administration (Figure 3B) (rat > dog ≫ monkey). Therefore, the present results verify that hydrolase activity in the small intestine in the process of absorption plays an important role in small intestinal first-pass metabolism after oral administration of a drug bearing an amide moiety. Furthermore, since the carboxylesterase isoform present in the small intestine is different from that in the liver and that OT-7100 is a good substrate for the carboxylesterase isoforms in monkey small intestines.

Since there are marked species variations in substrate specificity and tissue distribution of carboxylesterases, it is not yet possible to predict using animal studies all relevant aspects of drug metabolism and pharmacokinetics in human clinical studies involving administration of drugs with an amide moiety. However, the results presented here offer an important index to extrapolate drug metabolism and pharmacokinetics in humans from *in vitro* studies using both human and animal tissue fractions as well as animal studies. Particularly relevant is the observation that hydrolase activities toward OT-7100 in human liver microsomes were one-third to one-fifth lower than those in other species (Figure 4). Therefore, after intravenous administration to humans, OT-7100 should have a longer half-life and lower clearance in humans than in other animals. Our data indicate that the metabolism and pharmacokinetics of OT-7100 in humans would be sufficiently different such that the predicted bioavailabilities of this drug in humans would be higher than those in monkeys. In fact, it was confirmed that the plasma concentrations of OT-7100 in human volunteers normalized for dose concentration after oral administration were higher than those of monkeys (data not shown).

In conclusion, this paper has demonstrated that small intestinal hydrolysis in the process of absorption plays a crucial role in the first-pass metabolism of the OT-7100 after oral administration. Furthermore, OT-7100 is a good substrate for esterase isoforms in monkey small intestine and can therefore be a good probe drug to elucidate differences in small intestinal hydrolase activities between humans and monkeys. This information provides an important index for extrapolating human drug pharmacokinetics from preclinical monkey studies.

References

Boogaard PJ, Van Elburg PA, De Kloe KP, Watson WP, Van Sittert NJ. 1999. Metabolic inactivation of 2-oxiranylmethyl 2-ethyl-2,5-dimethylhexanoate (C10GE) in skin, lung and liver of human, rat and mouse. Xenobiotica 29:987–1006.

Boxenbaum H. 1980. Interspecies variation in liver weight, hepatic blood flow, and antipyrine intrinsic clearance: Extrapolation of data to benzodiazepines and phenytoin. Journal of Pharmacokinetics and Biopharmaceutics 8:165–176.

Campbell CJ, Chantrell LJ, Eastmond R. 1987. Purification and partial characterization of rat intestinal cefuroxime axetil esterase. Biochemical Pharmacology 36:2317–2324.

Cook CS, Karabatsos PJ, Schoenhard GL, Karim A. 1995. Species dependent esterase activities for hydrolysis of an anti-HIV prodrug glycovir and bioavailability of active SC-48334. Pharmaceutical Research 12:1158–1164.

Fitzsimmons ML, Collins JM. 1997. Selective biotransformation of the human immunodeficiency virus protease inhibitor Saquinavir by human small-intestinal cytochrome P4503A4. Potential contribution to high first-pass metabolism. Drug Metabolism and Disposition 25:256–266.

Hashizume T, Imaoka S, Mise M, Terauchi Y, Fujii T, Miyazaki H, Kamataki T, Funae Y. 2001. Involvement of CYP2J2 and CYP4F12 in the metabolism of ebastine in human intestinal microsomes. Journal Pharmacology and Experimental Therapeutics 300:298–304.

Hosokawa M, Endo T, Fujisawa M, Hara S, Iwata N, Sato Y, Satoh T. 1995. Interindividual variation in carboxylesterase levels in human liver microsomes. Drug Metabolism and Disposition 23:1022–1027.

Hosokawa M, Maki T, Satoh T. 1990. Characterization of molecular species of liver microsomal carboxylesterases of several animal species and humans. Archives of Biochemistry and Biophysics 277:219–227.

Hosokawa M, Suzuki K, Takahashi D, Mori M, Satoh T, Chiba K. 2001. Purification, molecular cloning, and functional expression of dog liver microsomal acyl-CoA hydrolase: A member of the carboxylesterase multigene family. Archives of Biochemistry and Biophysics 389:245–253.

Imai T, Yoshigae Y, Hosokawa M, Chiba K, Otagiri M. 2003. Evidence for the involvement of a pulmonary first-pass effect via carboxylesterase in the disposition of a propranolol ester derivative after intravenous administration. Journal of Pharmacology and Experimental Therapeutics 307:1234–1242.

Inaba M, Ohnishi Y, Ishii H, Tanioka Y, Yoshida Y, Sudoh K, Hakusui H, Mizuno N, Ito K, Sugiyama Y. 1998. Pharmacokinetics of CPT-11 in rhesus monkeys. Cancer Chemotherapy and Pharmacology 41:103–108.

Inoue M, Morikawa M, Tsuboi M, Sugiura M. 1979. Species difference and characterization of intestinal esterase on the hydrolyzing activity of ester-type drugs. Japanese Journal of Pharmacology 29:9–16.

Lin JH. 1995. Species similarities and differences in pharmacokinetics. Drug Metabolism and Disposition 23:1008–1021.

Lin JH, Chiba M, Baillie TA. 1999. Is the role of the small intestine in first-pass metabolism overemphasized? Pharmacological Reviews 51:135–158.

Lowry OH, Rosebrough NJ, Farr AL, Randall RJ. 1951. Protein measurement with the Folin phenol reagent. Journal of Biological Chemistry 193:264–275.

Miki S, Yoshinaga N, Iwamoto T, Yasuda T, Sato S. 2001. Antinociceptive effect of the novel compound OT-7100 in a diabetic neuropathy model. European Journal of Pharmacology 430:229–234.

Morgan EW, Yan B, Greenway D, Parkinson A. 1994a. Regulation of two rat liver microsomal carboxylesterase isozymes: Species differences, tissue distribution, and the effects of age, sex, and xenobiotic treatment of rats. Archives of Biochemistry and Biophysics 315:513–526.

Morgan EW, Yan B, Greenway D, Peterson DR, Parkinson A. 1994b. Purification and characterization of two rat liver microsomal carboxylesterases (hydrolase A and B). Archives of Biochemistry and Biophysics 31:495–512.

Satoh T. 1987, Role of carboxylesterases in xenobiotic metabolism. In: Bend JR, Hodgson E, Philpot RM, editors. New York, NY: Elsevier. pp 155–181.

Satoh T, Hosokawa M. 1998. The mammalian carboxylesterases: From molecules to functions. Annual Review of Pharmacology and Toxicology 38:257–288.

Thummel KE, Kunze KL, Shen DD. 1997. Enzyme-catalyzed processes of first-pass hepatic and intestinal drug extraction. Advanced Drug Delivery Reviews 27:99–127.

Thummel KE, O'Shea D, Paine MF, Shen DD, Kunze KL, Perkins JD, Wilkinson GR. 1996. Oral first-pass elimination of midazolam involves both gastrointestinal and hepatic CYP3A-mediated metabolism. Clinical Pharmacology and Therapeutics 59:491–502.

Yamaoka K, Nakagawa T, Uno T. 1978. Statistical moments in pharmacokinetics. Journal of Pharmacokinetics and Biopharmaceutics 6:547–558.

Yan B, Matoney L, Yang D. 1999. Human carboxylesterases in term placentae: Enzymatic characterization, molecular cloning and evidence for the existence of multiple forms. Placenta 20:599–607.

Yasuda T, Iwamoto T, Ohara M, Sato S, Kohri H, Noguchi K, Senba E. 1999. The novel analgesic compound OT-7100 (5-nButyl-7-(3,4,5,-trimethoxybenzoylamino)pyrazolo[1,5-a]pyrimidine) attenuates mechanical nociceptive responses in animal models of acute and peripheral neuropathic hyperalgesia. Japanese Journal of Pharmacology 79:65–73.

Yasuda T, Okamoto K, Iwamoto T, Miki S, Yoshinaga N, Sato S, Noguchi K, Senba E. 2001. A novel analgesic compound OT-7100 attenuates nociceptive responses in animal models of inflammatory and neuropathic hyperalgesia: A possible involvement of adenosinergic anti-nociception. Japanese Journal of Pharmacology 87:214–225.

Zhang QY, Dunbar D, Ostrowska A, Zeisloft S, Yang J, Kaminsky LS. 1999. Characterization of human small intestinal cytochromes P-450. Drug Metabolism and Disposition 27:804–809.

Zhang W, Xu G, McLeod HL. 2002. Comprehensive evaluation of carboxylesterase-2 expression in normal human tissues using tissue array analysis. Applied Immunohistochemistry and Molecular Morphology 10:374–380.

Zhu W, Song L, Zhang H, Matoney L, Lecluyse E, Yan B. 2000. Dexamethasone differentially regulates expression of carboxylesterase genes in humans and rats. Drug Metabolism and Disposition 28:186–191.

0026-895X/06/7002-477–486$20.00
MOLECULAR PHARMACOLOGY

Mol Pharmacol 70:477–486, 2006

Vol. 70, No. 2
22673/3125134
Printed in U.S.A.

CYP2C76, a Novel Cytochrome P450 in Cynomolgus Monkey, Is a Major CYP2C in Liver, Metabolizing Tolbutamide and Testosterone

Yasuhiro Uno, Hideki Fujino, Go Kito, Tetsuya Kamataki, and Ryoichi Nagata

Laboratories of Translational Research (Y.U., G.K., R.N.) and Drug Metabolism (T.K.), Graduate School of Pharmaceutical Sciences, Hokkaido University, Hokkaido, Japan; Shin Nippon Biomedical Laboratories, Tokyo, Japan (Y.U., G.K., R.N.); and Tokyo New Drug Research Laboratories I, Kowa Co., Tokyo, Japan (H.F.)

Received January 20, 2006; accepted April 21, 2006

ABSTRACT

Monkeys are widely used as a primate model to study drug metabolism because they generally show a metabolic pattern similar to humans. However, the paucity of information on cytochrome P450 (P450) genes has hampered a deep understanding of drug metabolism in the monkey. In this study, we report identification of the CYP2C76 cDNA newly identified in cynomolgus monkey and characterization of this CYP2C along with cynomolgus CYP2C20, CYP2C43, and CYP2C75. The CYP2C76 cDNA contains the open reading frame encoding a protein of 489 amino acids that are only approximately 80% identical to any human or monkey P450 cDNAs. Gene and protein expression of CYP2C76 was confirmed in the liver of cynomolgus and rhesus monkeys but not in humans or the great apes. Moreover, *CYP2C76* is located at the end of the *CYP2C* gene cluster in the monkey genome, the region of which corresponds to the intergenic region adjacent to the *CYP2C* cluster in the human genome, strongly indicating that this gene does not have the ortholog in humans. Among the four *CYP2C* genes expressing predominantly in the liver, the expression level of *CYP2C76* was the greatest, suggesting that CYP2C76 is a major CYP2C in the monkey liver. Assays for the capacity of CYP2C76 to metabolize drugs using several substrates typical for human CYP2Cs revealed that CYP2C76 showed unique metabolic activity. These results suggest that CYP2C76 contributes to overall drug-metabolizing activity in the monkey liver and might account for species difference occasionally seen in drug metabolism between monkeys and humans.

Cytochrome P450s (P450s) are one of the most important drug-metabolizing enzymes and form a superfamily consisting of a large number of subfamilies (Nelson et al., 1996, 2004). The cDNA sequences encoding P450s have been reported for many species of not only mammals but also birds, insects, plants, bacteria, and others (see http://drnelson.utmem.edu/CytochromeP450.html). In humans, 57 functional genes have been identified to date (Nelson et al., 2004). The human CYP2C subfamily, comprising CYP2C8, CYP2C9, CYP2C18, and CYP2C19, is essential in metabolizing approximately 20% of all prescribed drugs, including tolbutamide, phenytoin, warfarin, and ibuprofen (Goldstein, 2001). The CYP2C subfamily consists of multiple members in each mammalian species, including 15 in mice, 12 in rats, and 9 in rabbits (for the latest information, see http://drnelson.utmem.edu/CytochromeP450.html). Between humans and rodents, the number of the subfamily members is different, and none of the CYP2Cs seems to show a clear orthologous relationship between the two species, suggesting that the data from rodents must be cautiously interpreted and extrapolated to humans (Nelson et al., 2004).

For monkeys, which generally mean Old or New World monkeys, three CYP2C cDNAs have been identified in the macaque and cynomolgus (*Macaca fascicularis*) and rhesus (*Macaca mulatta*) monkeys. Two sequences have been published including cynomolgus CYP2C20 (Komori et al., 1992) and rhesus CYP2C43 (Matsunaga et al., 2002), whereas rhesus CYP2C75 has been reported to GenBank but unpublished. CYP2C20 shows ~95% homology to human CYP2C8, whereas CYP2C43 and CYP2C75 have ~95% identity to both human CYP2C9 and CYP2C19. Among these monkey CYP2Cs, only CYP2C43 has been analyzed for drug-metabolizing capacity using the recombinant protein, showing activities toward *S*-mephenytoin but not tolbutamide, similar

Article, publication date, and citation information can be found at http://molpharm.aspetjournals.org.
doi:10.1124/mol.106.022673.

ABBREVIATIONS: P450, cytochrome P450; PCR, polymerase chain reaction; BAC, bacterial artificial chromosome; RT, reverse transcription; TLC, thin-layer chromatography; PDI, protein disulfide isomerase; EST, expressed sequence tag; PTC, premature termination codon; NMD, nonsense-mediated decay.

to metabolic properties for human CYP2C19 (Matsunaga et al., 2002).

The monkey, the animal evolutionarily close to humans, shows not only phenotypic but also physiological similarities to humans in such biological circumstances as aging (Roth et al., 2004), reproduction (Bellino and Wise, 2003), and neurological disease, including Parkinson's disease (Takagi et al., 2005). This resemblance can be partly explained by a relatively high similarity (~97%) of protein sequences generally seen between monkeys and humans (Magness et al., 2005). For preclinical trials during drug development, monkeys, especially macaques, are used as a large and nonrodent species to evaluate drug effects because they generally show pharmacokinetics more similar to humans than any nonprimate models. However, it has become apparent that monkeys are not always similar to humans in drug metabolism (Stevens et al., 1993; Sharer et al., 1995; Guengerich, 1997; Weaver et al., 1999; Bogaards et al., 2000; Narimatsu et al., 2000). We hypothesized that this species difference was due to the difference in the genetic components essential for drug metabolism such as P450s between monkeys and humans. In monkeys, information on the characteristics of drug-metabolizing enzymes is largely scarce, especially at molecular level, preventing a deep understanding of drug metabolism. Therefore, to test our hypothesis, we have identified a number of the cynomolgus monkey cDNA clones for P450s; the characterization of these clones is currently ongoing. Successful drug development requires accuracy in the extrapolation of drug metabolism and toxicity data from experimental animals to humans. Then characterization of these cynomolgus P450s should help to better understand drug metabolism in monkeys.

In this article, we report the isolation and characterization of cynomolgus CYP2C76, a novel P450 with a low homology to any human or monkey CYP2C cDNAs. RT-PCR and immunoblotting indicated the expression of mRNA and protein homologous to CYP2C76 in cynomolgus and rhesus monkeys but not in humans. Moreover, the genomic analysis indicated that the *CYP2C76* gene was located at the end of the *CYP2C* cluster in the macaque genome, the location of which corresponded to an intergenic region in the human genome, suggesting that the P450 homologous to CYP2C76 does not exist in humans. The hepatic expression of CYP2C76 was higher than any other CYP2Cs analyzed, indicating that this P450 was a major CYP2C in the monkey liver. CYP2C76 protein was active in the metabolism of tolbutamide and testosterone. Because of its species specificity and functional importance, CYP2C76 might account for the species difference occasionally seen in drug metabolism between monkeys and humans.

Materials and Methods

Chemicals and Reagents. 4-Hydroxytolbutamide, 6α-hydroxypaclitaxel, 3-hydroxypaclitaxel, 4-hydroxy-*S*-mephenytoin, and 6β-hydroxytestosterone were purchased from Ultrafine Chemicals (Manchester, UK). Pooled hepatic microsomes from human subjects and male cynomolgus monkeys were both purchased from BD Gentest (Woburn, MA). Labeled [2-benzoyl ring-U-^{14}C]paclitaxel (2.23 MBq/mg) was obtained from Sigma-Aldrich (St. Louis, MO), whereas [ring-U-^{14}C]tolbutamide (2.26 GBq/mmol), *S*-[4-^{14}C]mephenytoin (9.42 MBq/mg), and [4-^{14}C]testosterone (2.11 GBq/mmol) were from GE Healthcare (Little Chalfont, Buckinghamshire, UK). The radiochemical purities of these ^{14}C-labeled chemicals were >99%. Oligonucleotides were synthesized by Sigma-Genosys (Ishikari, Japan). All other reagents were purchased from Sigma-Aldrich unless otherwise specified.

Tissue Samples and RNA Extraction. Tissue samples were collected from individual monkeys, including six cynomolgus monkeys (three male and three female) and two male rhesus monkeys, which were kept under the established guidelines and standard procedures at Shin Nippon Biomedical Laboratories (Tokyo, Japan). The study was approved by the local ethics committee. The tissue samples from brain, lung, heart, liver, kidney, adrenal gland, small intestine, testis, ovary, and uterus were frozen in liquid nitrogen right after removal from animals to prevent potential RNA degradation. Orangutan and chimpanzee liver samples were kindly provided by GAIN (Great Ape Information Network, Japan). The frozen tissues were first ground with mortar and pestle and then processed in TRIzol (Invitrogen, Carlsbad, CA) with a Polytron homogenizer (Kinematica, Basel, Switzerland), followed by extraction of total RNA according to the manufacturer's instruction. After treatment with DNase I (Takara, Tokyo, Japan), the RNA was purified using GenElute Mammalian Total RNA Mini Kit (Sigma-Aldrich).

Cell Culture and RNA Extraction. COS1 cells from the American Type Culture Collection (Manassas, VA) was cultured as described previously (Saito et al., 2001). RNA extraction from the cell and the subsequent DNase I treatment were performed using RNeasy Mini Kit (QIAGEN, Valencia, CA) according to the manufacturer's protocol.

Cloning of CYP2C76 Homologous cDNA in Other Primate Species. RNA was extracted from liver (for rhesus monkey, orangutan, and chimpanzee) and COS1 cell (for African green monkey). The first-strand cDNA was generated in a mixture containing 1 μg of total RNA, oligo (dT) or random primers, and Moloney murine leukemia virus reverse transcriptase (Toyobo, Osaka, Japan) at 37°C for 1 h. The resultant cDNA was diluted 25-fold and used as a template for the subsequent PCR. For human cDNA, the liver cDNA available from BD Biosciences (San Jose, CA) was used. The amplification was carried out using KOD Plus DNA polymerase (Toyobo) according to the manufacturer's protocol with the MJ Research thermal cycler (MJ Research, Watertown, CA). PCR conditions include an initial denaturation at 95°C for 2 min and 30 cycles of 95°C for 20 s, 55°C for 20 s, and 72°C for 2 min, followed by a final extension at 72°C for 10 min. Among several different primer-pairs tested, a CYP2C76 homologous sequence for rhesus and African green monkeys was successfully amplified by PCR using the following primer pairs: mf27B9 (5rt2), 5′-CCCAGCAATGGATCTCTTCA-3′, and mf27B9 (3polyA2a), 5′-TGCCTAGACAGGTAGATAGGAGTG-3′, for the rhesus monkey; mf27B9 (5rt2) and mf27B9 (3ex4b), 5′-GAAAAGTGGGATCACAGGGA-3′, for the African green monkey. After the addition of 3′ A-overhangs, the PCR products were cloned into vectors using TOPO TA Cloning Kit (Invitrogen). The inserts were then sequenced using ABI Prism BigDye Terminator v3.0 Ready Reaction Cycle Sequencing Kit (Applied Biosystems, Foster City, CA), followed by electrophoresis with the ABI Prism 3730 DNA Analyzer (Applied Biosystems).

Sequence Analysis. Raw sequence data were imported into DNASIS Pro (Hitachi Software, Tokyo, Japan) for most sequence analyses. After vector sequences and regions of sequence with unacceptable quality were removed, the trimmed sequences were assembled to the full-length sequence. A homology search was conducted by the BLAST program (National Center for Biotechnology Information). Multiple alignment of amino acid sequences was performed with the ClustalW program; the resultant alignment was used to create a phylogenetic tree using the PHYLIP program by default parameter. The human and chimpanzee genome data were searched for the sequence homologous to CYP2C76 by BLAT search (UCSC Genome Bioinformatics). Likewise, the macaque genome data (Baylor College of Medicine Human Genome Sequencing Center) were

used to identify and analyze the genome sequences corresponding to macaque CYP2Cs.

Amplification of CYP2C76 Introns. All the introns were amplified from cynomolgus monkey genomic DNA by PCR with 5 pmol each of forward and reverse gene-specific primers, 0.5 mM dNTPs, 2 mM $MgCl_2$, and 1 unit of LA *Taq* polymerase (Takara) in a total volume of 20 μl. The primers used to amplify introns 1 to 8 were mf27B9 (5rt2), mf27B9 (5ex2a), mf27B9 (5ex3a), mf27B9 (5ex4a), mf27B9 (5ex5a), mf27B9 (5ex6a), mf27B9 (5qrt1), or mf27B9 (5gen1) as a forward primer and mf27B9 (3ex2a), mf27B9 (3ex3a), mf27B9 (3ex4a), mf27B9 (3ex5a), mf27B9 (3ex6a), mf27B9 (3ex7a), mf27B9 (3qrt1), or mf27B9 (3rt1) as a reverse primer, respectively. The nucleotide sequence for each primer is listed below. Thermal cycler conditions were as follows: 95°C for 2 min; 35 cycles of 95°C for 20 s, 55°C for 30 s, and 72°C for 5 min; and a final extension at 72°C for 20 min. After electrophoresis in 0.8% agarose gels, the PCR products were gel-purified, cloned into vectors using TOPO XL Cloning Kit (Invitrogen), and sequenced. Sequencing and sequence analysis were performed as described above to determine the entire sequence of each intron.

The sequences of oligonucleotide primers used are as follows: mf27B9 (5ex2a), 5′-GTATTTTCTGGCCGAGGGAG-3′; mf27B9 (5ex3a), 5′-CGGCGTTTCTCTCTCATGGT-3′; mf27B9 (5ex4a), 5′-GGGTTGTGTTCCCTGTAATGTC-3′; mf27B9 (5ex5a), 5′-CATCAGGAATCTCTGGACATC-3′; mf27B9 (5ex6a), 5′-CAGAGACAACAAGCACCACAA-3′; mf27B9 (5qrt1), 5′-CCCATGCAGTGACTCAAGAC-3′; mf27B9 (5gen1), 5′-GCCACTTCCTGGACGAAAG-3′; mf27B9 (3ex2a), 5′-CTCCCTCGGCCAGAAAATAC-3′; mf27B9 (3ex3a), 5′-ATGCTTCCACCAGACACAAG-3′; mf27B9 (3ex4a), 5′-ACAGGGAACACAACCCAGAA-3′; mf27B9 (3ex5a), 5′-CGAGGGTTATTGATGTCCAGAG-3′; mf27B9 (3ex6a), 5′-GGAGCATCAGTCCATATCTCATT-3′; mf27B9 (3ex7a), 5′-ATTGGTGGGGATGAGGTCAATA-3′; mf27B9 (3qrt1), 5′-AAGTGGCCAGGGTCAAACT-3′; and mf27B9 (3rt1), 5′-ACAGCCTTGCTCTGCAATC-3′.

Isolation and Analysis of Monkey BAC Clones. The BAC clone containing the *CYP2C* genes was isolated by screening a rhesus monkey BAC library (BACPAC, Oakland, CA) using the CYP2C75 and CYP2C76 cDNAs as probes, because the BAC library was not available for cynomolgus monkeys. Hybridization with the library filters was carried out as recommended by the manufacturer using the probes synthesized in the presence of [α-^{32}P]dCTP (GE Healthcare) with the RadPrime DNA labeling system (Invitrogen). The identified BAC clones were obtained from the BACPAC. The BAC DNA was purified using DNA PhasePrep BAC DNA Kit (Sigma-Aldrich). To identify the *CYP2C* genes contained in each BAC DNA, the purified DNA was used as a template for the PCR with specific primers for 5′ or 3′ of each gene, 0.5 mM dNTPs, 2 mM MgCl2, and 1 unit of AmpliTaq Gold DNA polymerase (Applied Biosystems) in a total volume of 20 μl. PCR conditions were as follows: 95°C for 10 min; 30 cycles of 95°C for 20 s, 55°C for 20 s, and 72°C for 1 min; and final extension at 72°C for 10 min. The different primer pairs were initially designed at exons 1 and 9 of each gene, the location of which was determined by comparing each cynomolgus cDNA to the human *CYP2C* genes. For the genes highly homologous to *CYP2C43* and *CYP2C75*, the designed primers did not show a gene-specific amplification pattern. Therefore, the gene-specific indels were identified in introns 1 and 8 of these genes by searching the macaque genome data and the primers recognizing these indels were designed. The sequences of primers used for the PCR are listed in Table 1. The amplification pattern was examined to determine an arrangement of the *CYP2C* genes in the genome as described previously (Gray et al., 1995). For the same purpose, the DNA was also used for the BAC end sequencing and for a restriction enzyme mapping with BamHI or EcoRI as recommended by the BACPAC.

Real-Time RT-PCR. The primers and TaqMan MGB probes specific for each gene (Table 2) were designed using Primer Express software (Applied Biosystems). The 5′ end of the probes was labeled with 5-carboxyfluorescein fluorescence reporter dye. Reverse transcriptase reaction was carried out using random primers as described above. A twenty-fifth volume of the reaction mixture was then used for the subsequent PCR that was carried out in a total volume of 25 μl using TaqMan Universal PCR Master Mix (Applied Biosystems) with the ABI Prism 7700 sequence detection system (Applied Biosystems) following the manufacturer's protocol. Final concentration of each primer set was 0.3 μM for CYP2C20 and CYP2C43, 0.9 μM for CYP2C75, and 0.1 μM for CYP2C76. The final concentration of the probes was 0.25 μM for all CYP2Cs. Thermal cycler conditions for all reactions were 2 min at 50°C and 10 min at 95°C, followed by 40 cycles of 15 s at 95°C and 1 min at 60°C. Standard curves were generated by serial 10-fold dilutions of a plasmid for the corresponding cDNA. The specificity of assays for all *CYP2C* genes was confirmed by sequencing a single DNA band with the expected size in agarose gels and by performing the highly efficient amplification of cDNA plasmid for the target gene over that of the other *CYP2C* genes. Relative expression level of each gene was normalized to the 18S ribosomal RNA level measured using a predeveloped kit available from Applied Biosystems. At least three amplifications were performed for each gene.

Heterologous Expression of Four Recombinant CYP2Cs in *Escherichia coli*. Protein expression of the four CYP2Cs was carried out as described previously (Iwata et al., 1998). To enhance protein expression, the eight residues of the N terminus were replaced with the corresponding ones of the modified bovine CYP17, MALLLAVF (Barnes et al., 1991) by amplifying the open reading frame of each cDNA with the primers listed in Table 3 using the KOD Plus DNA polymerase. The forward and reverse primers contained

TABLE 1
Primers used for amplification of *CYP2C*-positive BAC clones

Gene	Sequence (5′→3′)	
	Forward	Reverse
CYP2C20		
5′	ATGGAACCTTTTGTGGTCCTG	GAAAGATTTGCAGATGTCCTTAAC
3′	TTTGTGCAGGAGAGGGACTT	ACGAGGGTGGCAGAGAAAT
CYP2C43		
5′	TCTTGAAGCTGGGTATTGGTC	AGGTGGATCACAAGGTCAGG
3′	GGATAAAATTATCCTCAAAATCCTC	CATCAAAGGTCACAGAATAAAGG
CYP2C75		
5′	TTGTTGCCTTTTCTCCATCA	CACGGTTAAACCATCTTTCACA
3′	GTTAAAGGAGATAATGAGCCACAG	GGAAAGATGTGTTTGCTTCCAC
CYP2C18-like		
5′	GTGAAAGCCCACAGTTTTCTTAC	CTCATGTCCTTAACATCTAACTGC
3′	TGACATCACCCCCATTGC	TGTGGGTTGACAAGTCAGAG
CYP2C76		
5′	CCCAGCAATGGATCTCTTCA	TGGCACCAAGCATTTATCTC
3′	CTTGCCTGTGTGTCAACCAT	ATTGGAATGGATTTTGAAGGA

NdeI and XbaI sites, respectively, so that after restriction enzyme digestion, the PCR products can be easily cloned into the pCW vector (Barnes, 1996), in which the human reductase cDNA has been already accommodated (Iwata et al., 1998). The resultant construct for CYP2C20, CYP2C43, CYP2C75, or CYP2C76 was used to transform DH5α competent cells (Invitrogen). Thereafter, sequence and orientation of each insert were confirmed by sequencing. To express proteins, the bacteria cells grown overnight in Luria-Bertani broth were diluted 100-fold and cultured in the presence of 200 μg/ml ampicillin for 6 to 12 h at 30°C in the modified Terrific broth (Iwata et al., 1998) until the optical density at 600 nm reached approximately 0.6 to 0.8. Isopropyl-β-D-thiogalactoside was then added to the culture at a final concentration of 1.5 mM. After 16 to 20 h, the cultured cells were harvested and cell membrane fraction was prepared as described previously (Daigo et al., 2002). The content of each CYP2C protein in the membrane preparation was determined by $Fe^{2+} \cdot CO$ versus Fe^{2+} difference spectra, according to the method described by Omura and Sato (1964) using the U-3000 spectrophotometer (Shimadzu, Kyoto, Japan). The concentration of NAPDH-P450 reductase was also measured as reported previously (Iwata et al., 1998; Daigo et al., 2002).

Drug-Metabolizing Activity of the Partially Purified Preparations of Monkey CYP2Cs. All the recombinant CYP2C proteins were analyzed for their activities to metabolize drugs with four substrates prototypical for human P450s, including paclitaxel, tolbutamide, *S*-mephenytoin, and testosterone. To prepare the reaction mixture, [^{14}C]paclitaxel (6 μM), [^{14}C]tolbutamide (100 μM), [^{14}C]*S*-mephenytoin (50 μM), or [^{14}C]testosterone (50 μM) was preincubated in a 100 mM sodium phosphate buffer solution, pH 7.4, with hepatic microsomes (1 mg/ml) or the partially purified recombinant CYP2Cs (200 pmol/ml) at 37°C for 5 min. This was followed by the addition of a NADPH regenerating system containing 1.3 mM $NADP^+$, 3.3 mM glucose 6-phosphate, 0.4 U/ml glucose-6-phosphate dehydrogenase, and 3.3 mM magnesium chloride in 100 mM sodium phosphate buffer, pH 7.4, so that the metabolic reaction was initiated at a final concentration of 1 mg of protein/ml or 200 pmol of P450/ml. After incubation at 37°C for 15 min (paclitaxel and testosterone), 45 min (*S*-mephenytoin), or 60 min (tolbutamide), the reaction was quenched by adding an equal volume of 100% methanol solution. For the recombinant CYP2Cs, the incubation was carried out for 30 min with all the tested substrates. The reaction-terminated samples were centrifuged, the aliquots of the supernatant were evaporated to dryness, and the residue was dissolved in 15 μl of methanol. The analysis of 6α-hydroxypaclitaxel and 3-hydroxypaclitaxel was performed as reported previously (Fujino et al., 2001). Aliquots (~2 μl) of the supernatant were spotted onto TLC plates (Silicagel 60F254, 20 × 20 cm; Merck, Darmstadt, Germany) and developed with toluene-acetone-formic acid [60:39:1 (v/v/v)] to 12 cm in a horizontal TLC chamber that was saturated with solvent vapor. The analysis of 6β-hydroxytestosterone was carried out as follows: supernatant was applied to TLC plates and developed with dichloromethane-acetone [4:1 (v/v)] to 16 cm. The measurement of 4-hydroxytolbutamide was performed as reported previously (Ludwig et al., 1998). In brief, the supernatant was spotted and developed with toluene-acetone-formic acid [60:39:1 (v/v/v)] to 10 cm. The assay for *S*-mephenytoin 4-hydroxylase activity was also performed according to a previous report (Shimada et al., 1985). The spotted supernatant was developed with chloroform-methanol-28% ammonium [90:10:1 (v/v/v)] to 12 cm. The TLC plates were dried and placed in contact with a phosphor imaging plate for 12 h. The amounts of unchanged drug and metabolites were determined using the BAS-2500 (Fuji Photo Film Co., Tokyo, Japan). The radioactive metabolites were positively identified by a comparison of R_f values using authentic unlabeled standard.

Immunoblotting. Polyclonal antibodies raised to CYP2C76 were produced by NeoMPS (San Diego, CA) using specific peptides for this protein. In brief, a peptide specific for CYP2C76 (Fig. 1) was designed, synthesized, purified, coupled through the terminal cysteine thiol with a keyhole limpet hemocyanin, and used to immunize New Zealand white rabbits. The recombinant P450 proteins (1.0 pmol each) were run in 10% SDS polyacrylamide gels and transferred to Hybond-P filters (GE Healthcare). The filters were immunoblotted with the rabbit anti-CYP2C76 (1:250) and the donkey anti-rabbit IgG conjugated with horseradish peroxidase (SantaCruz Biotechnology, Santa Cruz, CA). To detect protein disulfide isomerase (PDI) as a loading control, rabbit anti-PDI (1:200, SantaCruz Biotechnology) was also used. A specific band was visualized using an ECL Western blotting detection reagent (GE Healthcare) according to the manufacturer's instructions.

Immunohistochemistry. The sections of cynomolgus monkey liver were immunostained with the anti-CYP2C76 antibody after the standard procedure. In brief, the primary antibodies were diluted 50-fold and applied to the sections at 4°C overnight. The bound antibodies were detected using the EnVision+ System (Dako North America, Inc., Carpinteria, CA) and liquid diaminobenzidine (Dako North America) according to the manufacturer's instruction. Slides were counterstained with Harris hematoxylin. As a negative control, rabbit preimmune serum was used instead of primary antibodies. To validate immunohistochemical specificity, the antibodies were preincubated at 4°C overnight with excess amount of the CYP2C76

TABLE 2
Primers and probes used for real-time RT-PCR

Gene and Primer/Probe	Sequence (5′ → 3′)
CYP2C20	
Forward	TTTCTGGAAGAGGCATTTTGC
Reverse	TCCATCTCTTTCCATTGCTGG
Probe	AACGGACTTGGAATCA
CYP2C43	
Forward	GCCATTTCCCACTGTTTGAAA
Reverse	GCAGCGTCATGAGGGAGAA
Probe	ACAATTCCAAATCTTCT
CYP2C75	
Forward	TTCCATTGGCTGACAGAGCTAA
Reverse	CCGCAGTGTCATGAGGGAA
Probe	CGATTCCAAATCCT
CYP2C76	
Forward	TGGCCGAGGGAGTTTTCC
Reverse	AGAGAGAAACGCCGAATTTGC
Probe	CCAAGGATTCGGAGTTA

TABLE 3
Primers used to construct plasmids for protein expression
Bold letters show the modified N-terminal sequence, and underline indicates the NdeI or XbaI restriction site for forward or reverse primers, respectively.

cDNA and Direction	Sequence (5′ → 3′)
CYP2C20	
Forward	GGAATTCCATATGGCTCTGTTATTAGCAGTTTTTCTCTGTCTCTCCTTTGTGC
Reverse	GCTCTAGACAGATGGGCTAGCATTCTTCA
CYP2C43/CYP2C75	
Forward	GGAATTCCATATGGCTCTGTTATTAGCAGTTTTTCTCTGTCTCTCCTGTTTGC
Reverse	GCTCTAGACCAGACCATCTGCTCTTCTT
CYP2C76	
Forward	GGAATTCCATATGGCTCTGTTATTAGCAGTTTTTATTTGTCTTTCTTGTCTGAT
Reverse	GCTCTAGACTAGCAGCCAGACACTTCA

specific peptide (0.05 mg/ml) and this mixture was used in place of primary antibodies for immunohistochemistry.

Results

Identification of Cynomolgus CYP2C cDNAs. CYP2C76, along with CYP2C20, CYP2C43, and CYP2C75, was originally identified as a unique cDNA clone by searching our in-house EST database that was established using a full-length cDNA library prepared from the cynomolgus monkey liver (Y. Uno, Y. Suzuki, Y. Sakamoto, H. Sano, K. Hashimoto, S. Sugano, and I. Inoue, unpublished data). Among these, the se-quences newly identified in cynomolgus monkey, CYP2C43, CYP2C75, and CYP2C76, have been deposited to GenBank under accession numbers of DQ074806, DQ074805, and DQ074807, respectively. The CYP2C76 cDNA contained the open reading frame of 489 amino acids (Fig. 1). The deduced amino acid sequence showed primary sequence structures common to CYP2C molecules, including a highly hydrophobic N terminus, heme-binding region, and six potential substrate recognition sites (Gotoh, 1992). Blast analysis using the deduced amino acid sequences showed that CYP2C76 had only ~71% identity to any human CYP2Cs, whereas CYP2C20, CYP2C43, and CYP2C75 were ~92% homologous to human CYP2C (Table 4). This, together with a phylogenetic comparison of CYP2C amino acid sequences among mammalian species (Fig. 2), indicated possibilities that the CYP2C76 might be monkey-specific or that the human ortholog has not been isolated. To examine the latter possibility, we attempted to identify the sequence homologous to CYP2C76 in humans and other primate species by RT-PCR using gene-specific primer pairs. RNA samples used were from humans, the great apes (chimpanzee and orangutan), and Old World monkeys (cynomolgus, rhesus, and African green monkeys). The amplification was seen for Old World monkeys, and sequences of the PCR products were determined (data not shown). These CYP2C76 homologous sequences were ≥99% identical to each other, reflecting evolutionary closeness of these species. In contrast, the amplification with the human, chimpanzee, and orangutan samples showed no detectable bands in agarose gels (data not shown). Moreover, searching human and chimpanzee genome databases by BLAT (UCSC Genome Bioinformatics) showed no potential *CYP2C* genome sequence ≥90% homologous to the *CYP2C76*, raising the possibility that the CYP2C76 is monkey-specific.

Genomic Organization of the Monkey *CYP2C* Locus. To confirm the species specificity for CYP2C76, the location of the *CYP2C76* in the genome was determined by analyzing rhesus monkey CYP2C BAC clones. The *CYP2C*-positive clone was used for PCR as a template with gene-specific primers that were assigned at the 5′ and 3′ ends of each cynomolgus CYP2C cDNA. During the course of this study, the genome sequence data of the rhesus monkey became available and was used to confirm that the designed primers could be used for the rhesus monkey. The analysis of the data identified the genome sequence highly homologous to human *CYP2C18*. Therefore, the primers specific for this *CYP2C18*-like gene were also designed and used for amplification with the BAC clones. The amplification pattern of each gene, together with the end-sequencing and the restriction enzyme mapping of the BAC clones, indicated that the five *CYP2C*

TABLE 4
Amino acid identity among human and monkey CYP2Cs

	CYP2C20	CYP2C43	CYP2C75	CYP2C76
			%	
CYP2C8	92	78	76	70
CYP2C9	78	93	93	71
CYP2C18	77	81	81	72
CYP2C19	79	91	92	72
CYP2C20		78	77	70
CYP2C43			94	71
CYP2C75				71

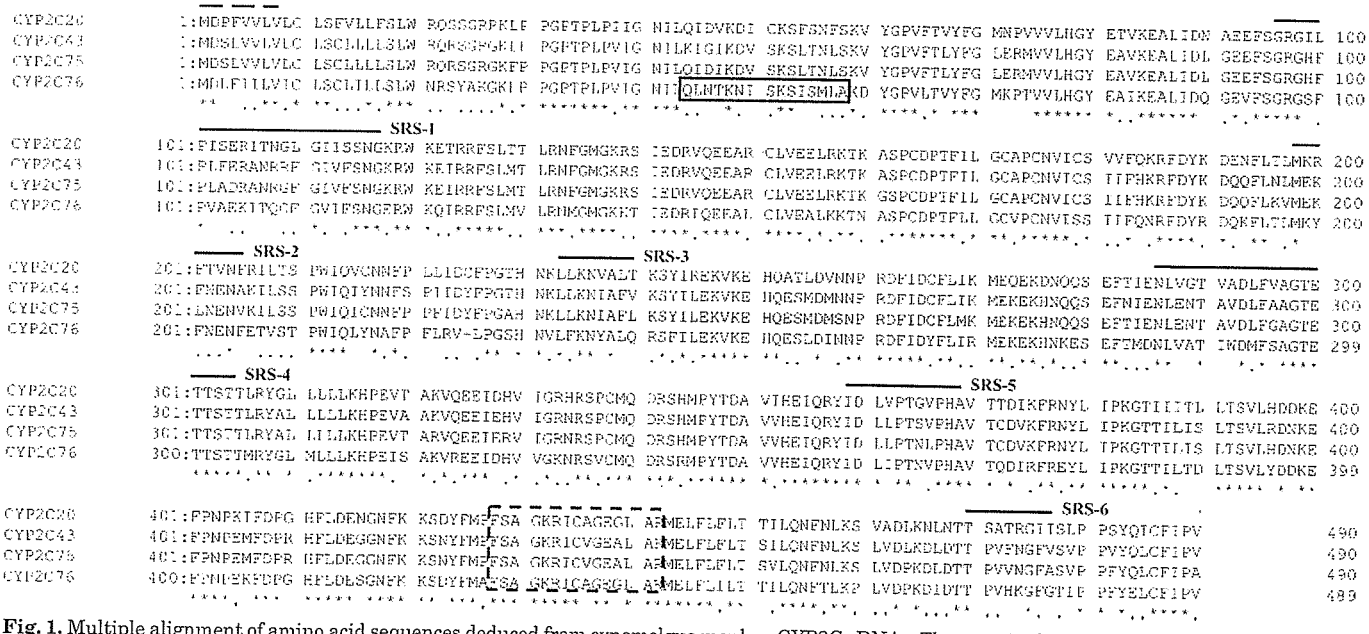

Fig. 1. Multiple alignment of amino acid sequences deduced from cynomolgus monkey CYP2C cDNAs. The putative heme-binding region characteristic of P450 protein is boxed with broken line. The broken and solid lines above the sequences indicate regions modified for protein expression and the six putative substrate recognition sites, respectively. The location of the peptide sequences used to raise the anti-CYP2C76 antibodies is boxed with solid line. Asterisks and dots under the sequences indicate identical amino acids and conservatively changed amino acids, respectively.

genes together form a gene cluster in the monkey genome similar to humans (Fig. 3). Moreover, *CYP2C76* was located at the end of the cluster, corresponding to the intergenic region adjacent to the *CYP2C* cluster in the human genome. These results strongly support the idea that *CYP2C76* is expressed in monkeys but not in humans.

Gene Structure of *CYP2C76*. To determine the gene structure of *CYP2C76*, long PCR amplification was performed with the genomic DNA of cynomolgus monkey as a template. Gene-specific primers were designed on each exon to amplify each intron. The sequences of the PCR products were determined as described above and assembled into the

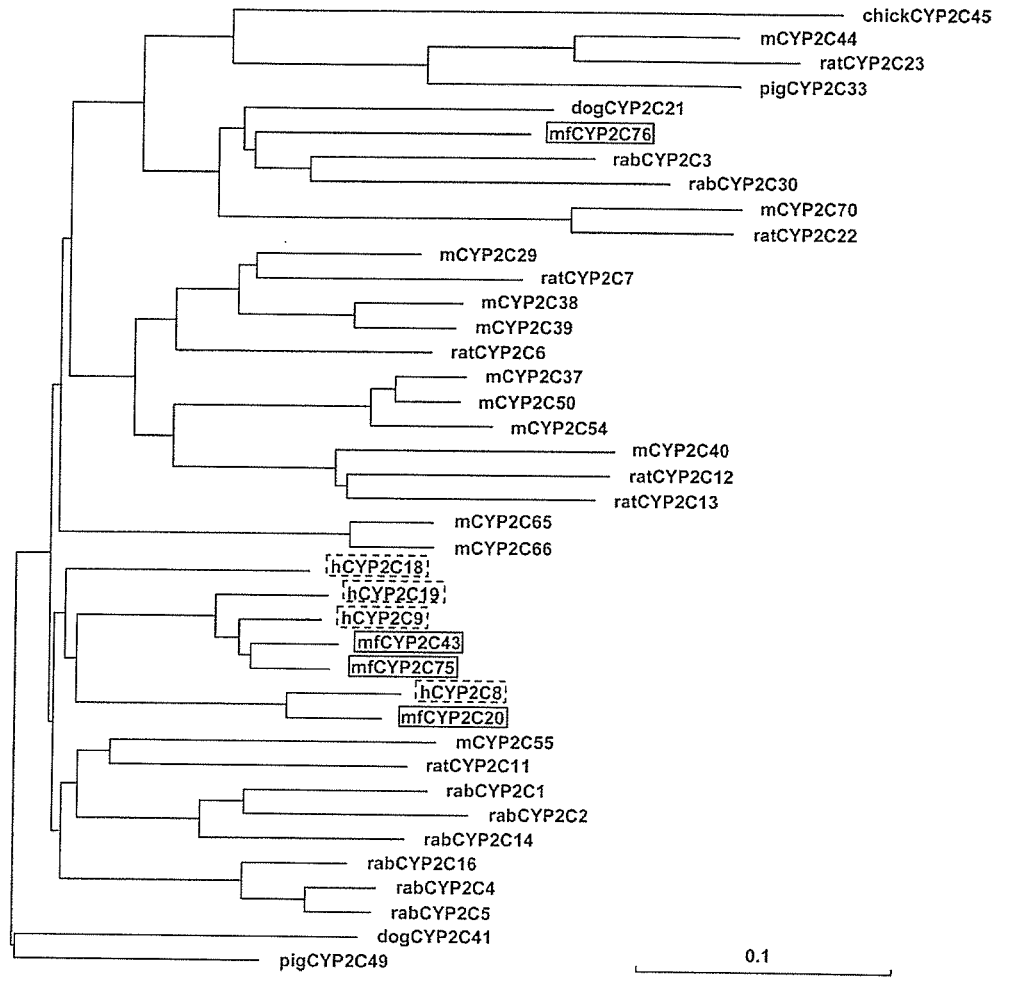

Fig. 2. Phylogeny of CYP2C amino acid sequences from cynomolgus monkey and other animal species. The phylogenetic tree was created using the Clustral W program. CYP2C amino acid sequences used were from cynomolgus monkey (mf), human (h), pig, dog, rabbit (rab), rat, mouse (m), and chicken (chick). The monkey and human CYP2Cs are boxed using solid and broken lines, respectively.

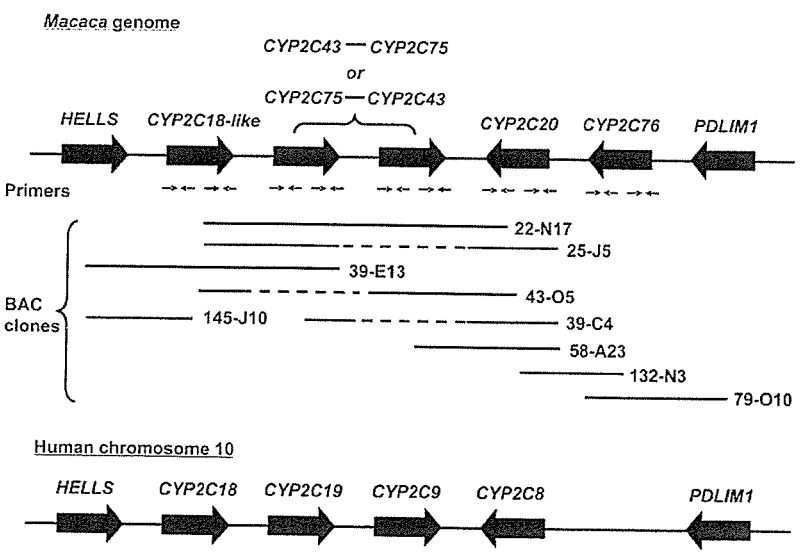

Fig. 3. Genomic structure of the monkey *CYP2C* genes. The *CYP2C* genes form the gene cluster in the macaque genome similar to the human genes as determined by PCR amplification patterns, and restriction enzyme mapping and end-sequencing of the *CYP2C*-positive BAC clones. Because an inter-relationship between *CYP2C43* and *CYP2C75* in the genome could not been clearly determined because of a high sequence homology of the two genes, the figure shows a tentative order of these genes. The broken lines indicate the regions of the BAC clones without a clear amplification, probably because of mispriming of the primers used.

entire intron. The *CYP2C76* gene spanned approximately 19.6 kb and contained nine exons, as has been described for all human *CYP2C* genes. Sizes of exons and introns ranged from 142 to 693 base pairs and from 937 to 4307 base pairs, respectively (Table 5). All exons were flanked by GU and AG dinucleotides consistent with the consensus sequences for splice junctions in eukaryotic genes, with the exception of the 5′ splice site for intron 8, where GU was replaced by GC.

Tissue Distribution of Gene Expression. To analyze the expression of cynomolgus *CYP2C20*, *CYP2C43*, *CYP2C75*, and *CYP2C76*, real-time RT-PCR was performed with gene-specific primers and TaqMan MGB probes using RNAs prepared from brain, lung, heart, liver, kidney, adrenal gland, small intestine, testis, ovary, and uterus. All the four *CYP2C* genes were expressed predominantly in the liver with some extrahepatic expression (Fig. 4). Among these CYP2Cs, the expression level of *CYP2C76* was the highest, indicating that CYP2C76 is a major CYP2C in the monkey liver.

Drug-Metabolizing Activities of Monkey Recombinant CYP2Cs. The activity of monkey CYP2Cs to metabolize drugs was characterized by incubating partially purified recombinant CYP2Cs with NADPH-regenerating system in the presence of the radiolabeled substrates typical for human CYP2Cs, paclitaxel, tolbutamide, *S*-mephenytoin, and testosterone. The results showed that CYP2C20 was involved only in the metabolism of paclitaxel among the four substrates examined, similar to the metabolic properties observed for human CYP2C8 (Fig. 5A). Tolbutamide was metabolized by CYP2C75 and CYP2C76 (Fig. 5B), whereas *S*-mephenytoin was only weakly metabolized by CYP2C43 and CYP2C75 (Fig. 5C). Testosterone was efficiently metabolized by all the four CYP2Cs except for CYP2C20, in which the metabolites generated were different (Fig. 5D). It is noteworthy that all three P450s capable of metabolizing testosterone generated one common but unknown metabolite. In addition, the 6β-hydroxylation of testosterone and the 3-hydroxylation of paclitaxel, both of which are mediated by CYP3A4 in humans, were not observed in the presence of CYP2Cs. Our results indicate that each monkey CYP2C has the characteristic substrate specificity.

Immunoblotting and Immunohistochemistry. The peptide specific for CYP2C76 was synthesized and used to raise anti-CYP2C76 antibodies. To investigate the specificity of the antibodies, immunoblotting was performed using the recombinant proteins, including monkey CYP2C20, CYP2C43, CYP2C75, and CYP2C76, in addition to human CYP2C8, CYP2C9, CYP2C18, and CYP2C19. Among these proteins, the antibodies detected a single ~50-kDa band only in CYP2C76 (Fig. 6A), indicating the immunospecificity of the antibodies. The immunoblotting for CYP2C76 was also carried out with liver microsomes prepared from five primate species: human, chimpanzee, orangutan, and cynomolgus and rhesus monkeys. A signal of the expected size was clearly detected only with liver microsomes from cynomolgus and rhesus monkeys (Fig. 6B), coincided well with the results of the gene expression pattern of *CYP2C76*.

To determine the cellular localization of the CYP2C76 protein, the cryosections prepared from the cynomolgus monkey liver were stained with the anti-CYP2C76 antibodies. Strong staining was seen in the cytoplasm of hepatocytes but not in the cells lining the bile duct or the vein (Fig. 7A). Little or no staining was seen after peptide blocking (Fig. 7B) or with preimmune serum (Fig. 7C), indicating that the staining was specific for CYP2C76.

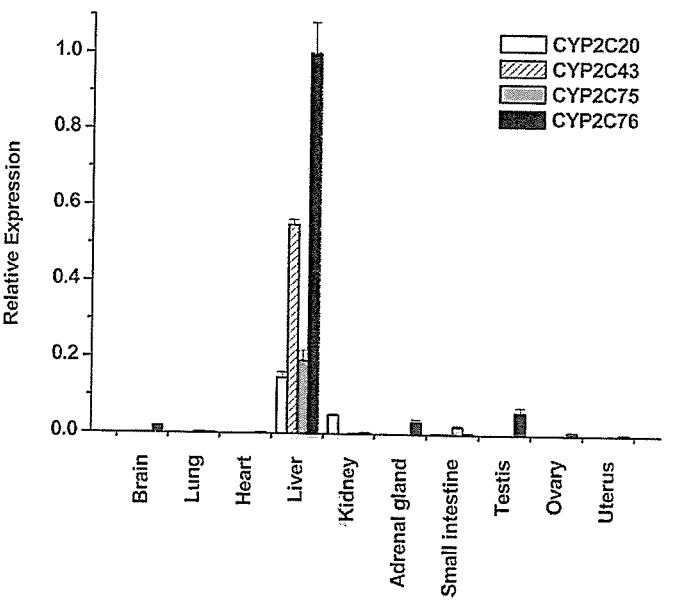

Fig. 4. Tissue distribution of *CYP2C* gene expressions in cynomolgus monkeys. Real-time RT-PCR was performed with each probe and primer set specific for *CYP2C20*, *CYP2C43*, *CYP2C75*, and *CYP2C76* using the RT products generated from total RNA of ten tissues. Expression level of each *CYP2C* gene was normalized to 18S rRNA level and represents the average ± S.D. from at least three independent experiments. For graphic representation, the expression level of *CYP2C76* for liver was adjusted to 1, and all other values were compared with the CYP2C76 level in liver.

TABLE 5

Sequences at each exon-intron boundary of *CYP2C76*

Exon and intron sequences are indicated in small and capital letters, respectively. The dinucleotide sequence at the highly conserved GU-AG motif is underlined.

Exon	Exon Size	3′ Splice Site	5′ Splice Site	Intron Size
	bp			*bp*
1	220		AAGCATGgtaagtatg	4148
2	163	tttttgcagCTAGCAA	GGATTCGgtatgcttc	1436
3	150	tgttgatagGAGTTAT	ACCAATGgtgtttgtt	2221
4	161	tgtttgtagCATCTCC	GATACAGgtaaggcca	1259
5	173	tcctttcagCTCTACA	GGAAAAGgtacaatgt	937
6	142	cattgctagGAAAAAC	ATCTCAGgtatgatca	1046
7	188	ccttgccagCTAAAGT	TCCAAAGgtgagagat	4307
8	142	ctttttcagGGCACAA	TCAGCAGgcaagcaag	2172
9	≥693	aatttttagGAAAAAG		

bp, base pairs.

Discussion

Monkeys have been employed in the preclinical studies of drug metabolism because they are believed to show a metabolic profile similar to that of humans. However, a different pattern is occasionally seen in drug metabolism between monkeys and humans (Stevens et al., 1993; Sharer et al., 1995; Guengerich, 1997; Weaver et al., 1999; Bogaards et al., 2000; Narimatsu et al., 2000). The molecular mechanism(s) behind this phenomenon remains unclear, partly as a result of the lack of detailed information on the genes and molecules responsible for drug metabolism in monkeys. In this study, to understand a possible cause responsible for this species difference, we identified a cDNA for CYP2C76 and characterized along with other CYP2C cDNAs encoding CYP2C20, CYP2C43, and CYP2C75 in cynomolgus monkeys. We investigated species specificity and tissue distribution of gene expression, in addition to genomic organization and metabolic properties.

The CYP2C subfamily has been known to be diverged in each species during evolution (Nelson et al., 1996, 2004), indicating that species specificity and orthologous relationship must be determined cautiously for the CYP2C subfamily. In this report, gene and protein expression pattern, genomic organization, and metabolic properties suggest that CYP2C76 does not seem to have the ortholog in humans. During the preparation of this article, a partial cDNA sequence for rhesus CYP2C76 was reported under GenBank accession number CX078602 as one of the clones identified by EST sequencing (Magness et al., 2005). In their report, PCR using gene-specific primers with the genomic DNA from several primate species showed the amplification in macaques but not in humans, further supporting our results. A definite conclusion could be made when a complete sequence of the monkey genome will be available.

The highly homologous *CYP2C* genes tend to be located near each other within the gene cluster, whereas *CYP2C44*, least homologous to other subfamily members, is located ~4 × 10^6 bases away from the mouse *CYP2C* gene cluster (Nelson et al., 2004). In contrast, *CYP2C76* (also least identical to any other *CYP2C* genes and thus placed outside the CYP2C group in the phylogenetic tree) is located within but on the edge of the *CYP2C* cluster in the monkey genome, similar to the mouse *CYP2C70* gene. The outer location probably did not allow *CYP2C76* for efficient crossover, resulting in the lower identity to other CYP2C subfamily members as has been proposed for *CYP2C44* and *CYP2C70* (Nelson et al., 2004). It is of great interest to know how *CYP2C76* has arisen after human and Old World monkeys diverged from a common ancestor around 25 million years ago (Kumar and Hedges 1998). Sequencing the *CYP2C* cluster of the closely related primate species should give an insight into this question.

Transcript variants influence the function of the P450 genes. Two transcript variants of *CYP4F3* contain either exon 3 or exon 4 generated through alternative splicing, leading to the high varieties of the synthesized proteins to accommodate different substrates as well as tissue specificity in gene expression (Christmas et al., 2001). In contrast, we identified a transcript variant for *CYP2C76* that lacks one of the exons, probably because of alternative splicing, which does not seem to have functional importance because of the premature termination codon (PTC) generated (data not

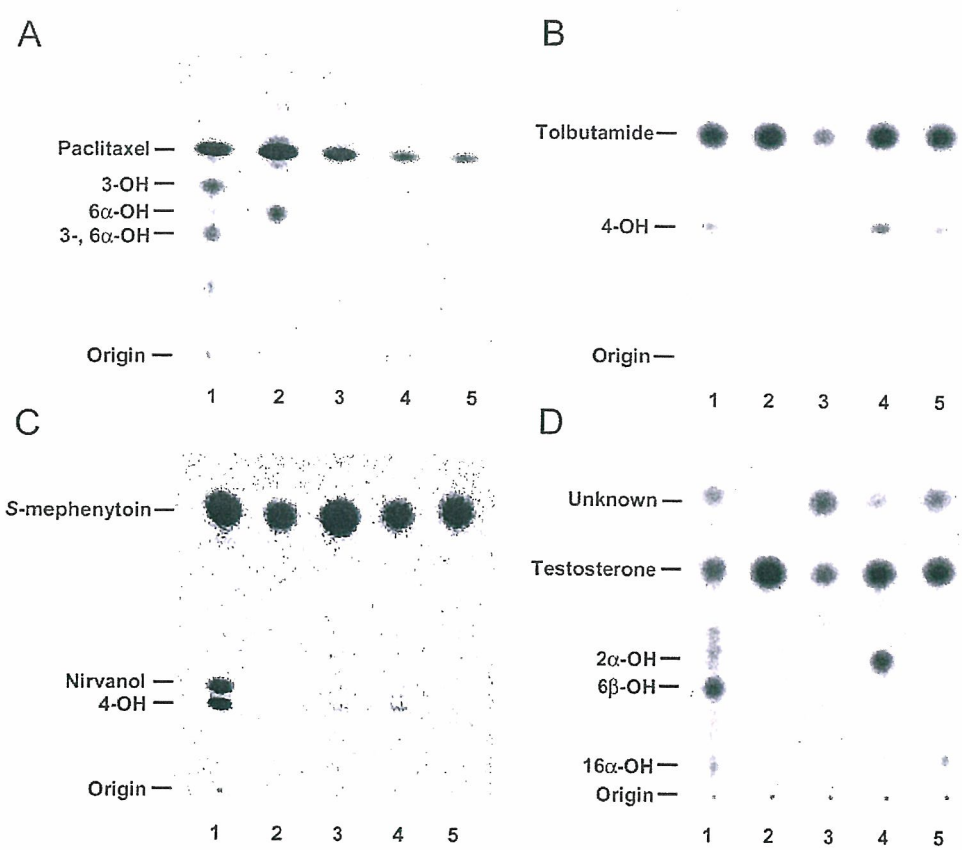

Fig. 5. High-performance liquid chromatography chromatograms after incubation of recombinant CYP2Cs with human CYP2C substrates. The reaction was performed using 1 mg/ml monkey hepatic microsomes or 200 pmol/ml the recombinant P450 in the presence of 6 μM paclitaxel (A), 100 μM tolbutamide (B), 50 μM *S*-mephenytoin (C), or 50 μM testosterone (D). The incubation time was 15 and 60 min for the microsomes and 30 min for the recombinants, respectively. Lanes 1 to 5 indicate the monkey hepatic microsomes, CYP2C20, CYP2C43, CYP2C75, and CYP2C76, respectively. Results are representative of three independent experiments.

shown). The PTC mRNAs can be subjected to a rapid degradation by nonsense-mediated decay (NMD) when PTCs are located more than 50 nucleotides before the last exon-exon junction (Holbrook et al., 2004). NMD is responsible for the degradation of the transcript variants generated by the *CYP3A5*3* allele, which can explain the difference in the expression levels of mRNAs between this and other genotype groups (Kuehl et al., 2001; Busi and Cresteil, 2005). Moreover, at least one third of alternative transcripts in humans were identified as PTC mRNAs, potential targets for RNA decay pathway through NMD (Lewis et al., 2003). Because gene expression is not completely diminished by NMD, expression levels remained would vary considerably between RNA isoforms, cell types, and even individuals (Holbrook et al., 2004). Therefore, together with the effect of SNPs on alternative splicing, the transcript variant of *CYP2C76* we identified, if subjected to NMD, could increase functional complexity of this gene.

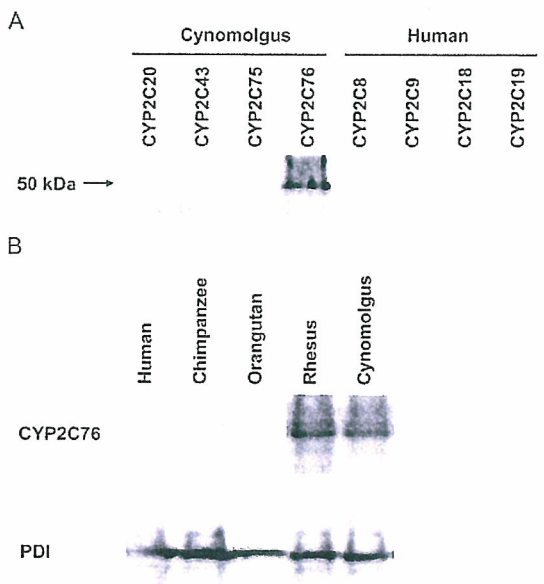

Fig. 6. Immunoblotting using the anti-CYP2C76 antibodies. The recombinant P450s (1.0 pmol of P450/lane) or liver microsomes (15 μg) were electrophoresed, transferred to polyvinylidene difluoride filters, and immunoblotted using anti-CYP2C76 antibodies. Each figure shows the representative image of three independent experiments. A, to investigate the specificity of the anti-CYP2C76 antibodies, the recombinant P450s were analyzed, including CYP2C20, CYP2C43, CYP2C75, and CYP2C76 for cynomolgus monkeys, and CYP2C8, CYP2C9, CYP2C18, and CYP2C19 for humans. B, to examine the presence of CYP2C76-homologous protein in other primate species, immunoblotting was performed with liver microsomes from humans, chimpanzee, orangutan, and rhesus and cynomolgus monkeys. PDI was used as a loading control.

CYP2C76 showed characteristic metabolic properties compared with CYP2C20, CYP2C43, and CYP2C75. CYP2C76 was critically involved in the metabolism of tolbutamide and testosterone, the metabolic properties of which are different from the other monkey CYP2Cs analyzed. CYP2C76, as a species-specific CYP2C enzyme, certainly adds the complexity to drug metabolism in monkeys and might account for the species difference in drug metabolism between monkeys and humans. Indeed, we have revealed that the CYP2C76 is at least partly responsible for the difference between monkeys and humans in the metabolism of a currently prescribed drug (Y. Uno, Y. Suzuki, Y. Sakamoto, H. Sano, K. Hashimoto, S. Sugano, and I. Inoue, unpublished observations). Further investigation of CYP2C76 on metabolic activity for a variety of substrates will help to better understand drug metabolism in monkeys and species difference between monkeys and humans.

The species difference of drug metabolism has been a major issue in drug development, because the results obtained with experimental animals need to be extrapolated to humans. The analysis for the capacity of hepatic microsomes from several animal species to metabolize drugs revealed that some differences occur in monkeys for the metabolism of marker substrates compared with humans (Sharer et al., 1995; Weaver et al., 1999; Bogaards et al., 2000). Tolbutamide hydroxylase activity is at least 3-fold lower in cynomolgus monkeys than humans (Sharer et al., 1995; Weaver et al., 1999), in contrary to our expectation because of monkey CYP2C75 and CYP2C76 exhibiting activities toward this substrate. This discrepancy might be due to the lower enzymatic activities of these enzymes compared with CYP2C9. However, other factors also need to be considered, such as genetic polymorphisms in individuals, from which the cDNA sequence used for protein expression was derived, because as in humans, monkeys have a diverse genetic background. Considering that even a single amino acid substitution can alter the enzymatic activity of P450s (Guengerich, 1997), nonsynonymous single nucleotide polymorphisms might have reduced the activity of CYP2C75 and CYP2C76. To examine this possibility, the genetic polymorphisms in *CYP2C76* and other *CYP2C* genes must be identified and characterized.

Understanding the species difference and the mechanisms behind it is an inevitable task to improve the accuracy in extrapolating the animal data to humans. To accomplish this goal, advancing genomic techniques such as EST or genome

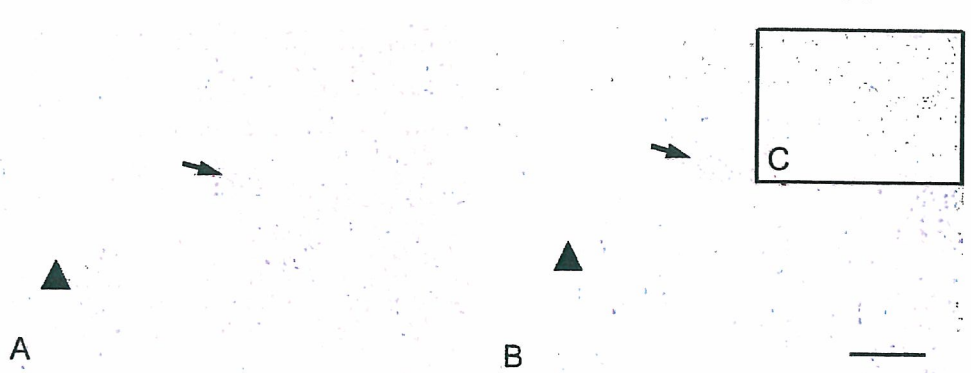

Fig. 7. Immunohistochemical staining of CYP2C76 protein in the liver. Sections were immunostained with anti-CYP2C76 antibodies (A), anti-CYP2C76 antibodies preincubated with blocking peptide (B), or preimmune serum (C). Strong positive staining was observed in hepatocytes, but not in the cells lining the bile duct (arrow) or the vein (arrowhead). Little or no staining was observed after peptide blocking or with preimmune serum. Results are representative of two independent experiments. The magnification is 20× for all pictures. The scale shown by solid line indicates 100 μm.

sequencing, microarray, and comparative genomics should be helpful because they can identify genomic components specific for each animal species including genes, transcripts, and regulatory elements. The ESTs specific for cynomolgus and rhesus monkeys have been identified by our and other groups (Magness et al., 2005), including *CYP2C76*. Further identification and characterization of monkey-specific ESTs will help to better understand the species uniqueness of monkeys in drug metabolism.

In conclusion, we have identified cynomolgus CYP2C76, which does not have the corresponding gene in the human genome. *CYP2C76* contains nine exons and is located in a single *CYP2C* cluster in the monkey genome, similar to the human *CYP2C* genes. Our data show that *CYP2C76* is predominantly expressed in the liver, and its expression level is the greatest among the four *CYP2C* genes analyzed. Moreover, CYP2C76 has a characteristic metabolic profile different from the other CYP2Cs. From these observations, we conclude that cynomolgus CYP2C76 is a major CYP2C contributing substantially to overall drug-metabolizing activity in the liver.

Acknowledgments

We thank the GAIN for providing us invaluable tissue samples from orangutan and chimpanzee, and Ms. Makiko Hase (Applied Biosystems) for assistance in designing gene-specific primers and probes for real-time RT-PCR. We also would like to acknowledge Dr. Aleksandar Milosavljevic at the Baylor College of Medicine for allowing us to access invaluable information on the rhesus monkey genome.

References

Barnes HJ (1996) Maximizing expression of eukaryotic cytochrome P450s in Escherichia coli. *Methods Enzymol* **272**:3–14.

Barnes HJ, Arlotto MP, and Waterman MR (1991) Expression and enzymatic activity of recombinant cytochrome P450 17 alpha-hydroxylase in Escherichia coli. *Proc Natl Acad Sci USA* **88**:5597–5601.

Bellino FL and Wise PM (2003) Nonhuman primate models of menopause workshop. *Biol Reprod* **68**:10–18.

Bogaards JJ, Bertrand M, Jackson P, Oudshoorn MJ, Weaver RJ, van Bladeren PJ, and Walther B (2000) Determining the best animal model for human cytochrome P450 activities: a comparison of mouse, rat, rabbit, dog, micropig, monkey and man. *Xenobiotica* **30**:1131–1152.

Busi F and Cresteil T (2005) CYP3A5 mRNA degradation by nonsense-mediated mRNA decay. *Mol Pharmacol* **68**:808–815.

Christmas P, Jones JP, Patten CJ, Rock DA, Zheng Y, Cheng SM, Weber BM, Carlesso N, Scadden DT, Rettie AE, et al. (2001) Alternative splicing determines the function of CYP4F3 by switching substrate specificity. *J Biol Chem* **276**: 38166–38172.

Daigo S, Takahashi Y, Fujieda M, Ariyoshi N, Yamazaki H, Koizumi W, Tanabe S, Saigenji K, Nagayama S, Ikeda K, et al. (2002) A novel mutant allele of the CYP2A6 gene (CYP2A6*11) found in a cancer patient who showed poor metabolic phenotype towards tegafur. *Pharmacogenetics* **12**:299–306.

Fujino H, Yamada I, Shimada S, and Yoneda M (2001) Simultaneous determination of taxol and its metabolites in microsomal samples by a simple thin-layer chromatography radioactivity assay—inhibitory effect of NK-104, a new inhibitor of HMG-CoA reductase. *J Chromatogr B Biomed Sci Appl* **757**:143–150.

Goldstein JA (2001) Clinical relevance of genetic polymorphisms in the human CYP2C subfamily. *Br J Clin Pharmacol* **52**:349–355.

Gotoh O (1992) Substrate recognition sites in cytochrome P450 family 2 (CYP2) proteins inferred from comparative analyses of amino acid and coding nucleotide sequences. *J Biol Chem* **267**:83–90.

Gray IC, Nobile C, Muresu R, Ford S, and Spurr NK (1995) A 2.4-megabase physical map spanning the CYP2C gene cluster on chromosome 10q24. *Genomics* **28**:328–332.

Guengerich FP (1997) Comparisons of catalytic selectivity of cytochrome P450 subfamily enzymes from different species. *Chem Biol Interact* **106**:161–182.

Holbrook JA, Neu-Yilik G, Hentze MW, and Kulozik AE (2004) Nonsense-mediated decay approaches the clinic. *Nat Genet* **36**:801–808.

Iwata H, Fujita K, Kushida H, Suzuki A, Konno Y, Nakamura K, Fujino A, and Kamataki T (1998) High catalytic activity of human cytochrome P450 co-expressed with human NADPH-cytochrome P450 reductase in Escherichia coli. *Biochem Pharmacol* **55**:1315–1325.

Komori M, Kikuchi O, Sakuma T, Funaki J, Kitada M, and Kamataki T (1992) Molecular cloning of monkey liver cytochrome P-450 cDNAs: similarity of the primary sequences to human cytochromes P-450. *Biochim Biophys Acta* **1171**:141–146.

Kuehl P, Zhang J, Lin Y, Lamba J, Assem M, Schuetz J, Watkins PB, Daly A, Wrighton SA, Hall SD, et al. (2001) Sequence diversity in CYP3A promoters and characterization of the genetic basis of polymorphic CYP3A5 expression. *Nat Genet* **27**:383–391.

Kumar S and Hedges SB (1998) A molecular timescale for vertebrate evolution. *Nature (Lond)* **392**:917–920.

Lewis BP, Green RE, and Brenner SE (2003) Evidence for the widespread coupling of alternative splicing and nonsense-mediated mRNA decay in humans. *Proc Natl Acad Sci USA* **100**:189–192.

Ludwig E, Wolfinger H, and Ebner T (1998) Assessment of microsomal tolbutamide hydroxylation by a simple thin-layer chromatography radioactivity assay. *J Chromatogr B Biomed Sci Appl* **707**:347–350.

Magness CL, Fellin PC, Thomas MJ, Korth MJ, Agy MB, Proll SC, Fitzgibbon M, Scherer CA, Miner DG, Katze MG, et al. (2005) Analysis of the *Macaca mulatta* transcriptome and the sequence divergence between Macaca and human. *Genome Biol* **6**:R60.

Matsunaga T, Ohmori S, Ishida M, Sakamoto Y, Nakasa H, and Kitada M (2002) Molecular cloning of monkey CYP2C43 cDNA and expression in yeast. *Drug Metab Pharmacokinet* **17**:117–124.

Narimatsu S, Kobayashi N, Masubuchi Y, Horie T, Kakegawa T, Kobayashi H, Hardwick JP, Gonzalez FJ, Shimada N, Ohmori S, et al. (2000) Species difference in enantioselectivity for the oxidation of propranolol by cytochrome P450 2D enzymes. *Chem Biol Interact* **127**:73–90.

Nelson DR, Koymans L, Kamataki T, Stegeman JJ, Feyereisen R, Waxman DJ, Waterman MR, Gotoh O, Coon MJ, Estabrook RW, et al. (1996) P450 superfamily: update on new sequences, gene mapping, accession numbers and nomenclature. *Pharmacogenetics* **6**:1–42.

Nelson DR, Zeldin DC, Hoffman SM, Maltais LJ, Wain HM, and Nebert DW (2004) Comparison of cytochrome P450 (CYP) genes from the mouse and human genomes, including nomenclature recommendations for genes, pseudogenes and alternative-splice variants. *Pharmacogenetics* **14**:1–18.

Omura T and Sato R (1964) The carbon monoxide-binding pigment of liver microsomes. II. Solubilization, purification and properties. *J Biol Chem* **239**:2379–2385.

Roth GS, Mattison JA, Ottinger MA, Chachich ME, Lane MA, and Ingram DK (2004) Aging in rhesus monkeys: relevance to human health interventions. *Science (Wash DC)* **305**:1423–1426.

Saito T, Takahashi Y, Hashimoto H, and Kamataki T (2001) Novel transcriptional regulation of the human CYP3A7 gene by Sp1 and Sp3 through nuclear factor kappa B-like element. *J Biol Chem* **276**:38010–38022.

Sharer JE, Shipley LA, Vandenbranden MR, Binkley SN, and Wrighton SA (1995) Comparisons of phase I and phase II in vitro hepatic enzyme activities of human, dog, rhesus monkey and cynomolgus monkey. *Drug Metab Dispos* **23**:1231–1241.

Shimada T, Shea JP, and Guengerich FP (1985) A convenient assay for mephenytoin 4-hydroxylase activity of human liver microsomal cytochrome P-450. *Anal Biochem* **147**:174–179.

Stevens JC, Shipley LA, Cashman JR, Vandenbranden M, and Wrighton SA (1993) Comparison of human and rhesus monkey in vitro phase I and phase II hepatic drug metabolism activities. *Drug Metab Dispos* **21**:753–760.

Takagi Y, Takahashi J, Saiki H, Morizane A, Hayashi T, Kishi Y, Fukuda H, Okamoto Y, Koyanagi M, Ideguchi M, et al. (2005) Dopaminergic neurons generated from monkey embryonic stem cells function in a Parkinson primate model. *J Clin Investig* **115**:102–109.

Weaver RJ, Dickins M, and Burke MD (1999) A comparison of basal and induced hepatic microsomal cytochrome P450 monooxygenase activities in the cynomolgus monkey (*Macaca fascicularis*) and man. *Xenobiotica* **29**:467–482.

Address correspondence to: Yasuhiro Uno, Laboratory of Translational Research, Graduate School of Pharmaceutical Sciences, Hokkaido University, Kita 14 Nishi 6, Kita-ku, Sapporo, 060-0812, Japan. E-mail: unoxx001@pharm.hokudai.ac.jp